

Precision measurements for the Higgsploding Standard Model

Valentin V. Khoze, Joey Reiness, Michael Spannowsky, and Philip Waite

Institute for Particle Physics Phenomenology, Department of Physics, Durham University, Durham, DH1 3LE, UK

E-mail: valya.khoze@durham.ac.uk, joey.y.reiness@durham.ac.uk,
michael.spannowsky@durham.ac.uk, p.a.waite@durham.ac.uk

ABSTRACT: Higgspllosion is the mechanism that leads to exponentially growing decay rates of highly energetic particles into states with very high numbers of relatively soft Higgs bosons. In this paper we study quantum effects in the presence of Higgspllosion. First, we provide a non-perturbative definition of Higgspllosion as a resolved short-distance singularity of quantum propagators at distances shorter than the inverse Higgspllosion energy scale, E_* . We then consider quantum effects arising from loops in perturbation theory with these propagators on internal lines. When the loop momenta exceed the Higgspllosion scale E_* , the theory dynamics deviates from what is expected in the standard QFT settings without Higgspllosion. The UV divergences are automatically regulated by the Higgspllosion scale, leading to the change of slopes for the running couplings at the RG scales $\mu > E_*$. Thus, the theory becomes asymptotically safe. Further, we find that the finite parts are also modified and receive power-suppressed corrections in $1/E_*^2$. We use these results to compute a set of precision observables for the Higgsploding Standard Model. These and other precision observables could provide experimental evidence and tests for the existence of Higgspllosion in particle physics.

Contents

1	Introduction	1
2	The propagator and Higgsplosion basics	2
2.1	The Dyson propagator	2
2.2	Continuation to Euclidean space	5
2.3	Multi-particle decay width	6
2.4	Where is Higgspersion in the semi-classical calculation?	9
2.5	The Higgsplosion scale E_*	13
2.6	Comment on the possibility of non-analytic corrections in ε to the large- n WKB amplitudes	15
3	Systematics of loops with Higgspersion	17
3.1	Computing a loop with the propagator in the classical background	17
3.2	Running couplings	24
3.3	Spontaneously broken theory	26
3.4	Exponentiation of the one-loop corrections	26
4	Precision observables in the presence of Higgsplosion	27
4.1	Propagators for fermions and massive vector bosons	27
4.2	Loop calculations for observables in the Standard Model	28
4.3	Procedure for Higgsplosion modifications to loop calculations	30
4.4	Results for precision observables	31
4.5	Higgs precision observables	32
4.6	Flavor observables	34
4.7	Anomalous magnetic dipole moment of the electron and muon	35
5	Discussion and Conclusions	36

1 Introduction

A conventional wisdom is that in the description of nature based on a local quantum field theory, one should always be able to probe shorter and shorter distances with higher and higher energies. Specifically, the characteristic length scales probed are $\Delta x \sim 1/E$ where E is the energy scale, a momentum transfer, or the virtuality that is achieved in the experiment. In the asymptotic regime where $E \rightarrow \infty$, one expects to probe $\Delta x \rightarrow 0$.

Higgsplosion [1] is a dynamical mechanism, or a new phase of the theory, which presents an obstacle to this length-scale/energy principle at energies above a certain value E_* , referred to as the Higgsplosion energy scale. Beyond this energy scale the dynamics of the

system is changed drastically [2]: distance scales below $|x| \lesssim 1/E_*$ cannot be resolved in interactions; UV divergences are regulated and the theory becomes asymptotically safe. This effect can also be depicted in the short-distance scaling behaviour of the propagator of a scalar particle,

$$\Delta(x) := \langle 0 | T(\phi(x) \phi(0)) | 0 \rangle \sim \begin{cases} m^2 e^{-m|x|} & : \text{for } |x| \gg 1/m \\ 1/|x|^2 & : \text{for } 1/E_* \ll |x| \ll 1/m \\ E_*^2 & : \text{for } |x| \lesssim 1/E_* \end{cases} \quad (1.1)$$

where for $|x| \lesssim 1/E_*$ one enters the Higgslosion regime.

In the simplest settings described by a quantum field theory of a massive scalar field ϕ with mass m and coupling λ , we show in Section 2 how Eq. (1.1) is linked to the growing multi-particle decay rates. Furthermore, we show that the Higgslosion energy scale is set by $E_* = C \frac{m}{\lambda}$, where C is a model-dependent constant of $\mathcal{O}(100)$. This expression holds in the weak-coupling limit $\lambda \rightarrow 0$. In this respect, it resembles the $SU(2)$ sphaleron, which has a mass scale of $M_{\text{sph}} = \text{const} \frac{m_W}{\alpha_w}$ [3, 4]. However, while the sphaleron is a phenomenon of the non-Abelian gauge-Higgs sector of the Standard Model, Higgslosion arises due to its scalar sector only.

The fundamental ingredient for the theory is the value of the Higgslosion scale E_* . It is the scale where the rate for the process $1^* \rightarrow n \times h$ grows exponentially for large enough n . The factorial growth of the rate has been calculated before at leading order [5–8], one-loop resummed [8–11], or using a semi-classical approach [12–15]. However, Higgslosion itself has not been taken into account in those calculations. Thus, in Section 3, we extend their approach by including Higgslosion, and, for the first time, calculate the loop-corrected rates in a self-consistent way.

After the Higgslosion scale E_* is established we can evaluate its phenomenological impact on precision observables, such as $gg \rightarrow h^{(*)}$, $h \rightarrow \gamma\gamma$, $h \rightarrow Z\gamma$, $B \rightarrow X_s\gamma$ or $g \rightarrow 2$. We calculate these precision observables explicitly in Section 4, and conclude with a discussion of our findings in Section 5.

2 The propagator and Higgslosion basics

2.1 The Dyson propagator

In the introduction we pointed out that the central object in a theory with Higgslosion is the propagator (1.1), and that Higgslosion manifests itself in resolving the short-distance singularity at $x^2 \leq 1/E_*^2$, where E_* is the characteristic (high-)energy scale of Higgslosion. To explain what we mean by this and how the effect of Higgslosion modifies the familiar structure of the propagator, it is worthwhile first to summarise the basic elements and the interplay between the propagator for a massive scalar field ϕ , its self-energy $\Sigma(p^2)$, and the partial width $\Gamma_n(p^2)$. This is the aim of this section.

Our technical discussion in this and the following section will be for a quantum field theory of a single massive scalar degree of freedom. The specific models we consider are the ϕ^4 theory with the unbroken Z_2 symmetry,

$$\mathcal{L} = \frac{1}{2} \partial^\mu \phi \partial_\mu \phi - \frac{1}{2} m_0^2 \phi^2 - \frac{\lambda}{4} \phi^4, \quad (2.1)$$

and a similar model with spontaneous symmetry breaking (SSB), where the scalar field has a non-zero VEV $\langle \phi \rangle = v$,

$$\mathcal{L} = \frac{1}{2} \partial^\mu \phi \partial_\mu \phi - \frac{\lambda}{4} (\phi^2 - v^2)^2, \quad (2.2)$$

$$\phi(x) = v + h(x), \quad m_h = \sqrt{2\lambda} v. \quad (2.3)$$

In the SSB case (2.2)-(2.3), m_h is the mass of the physical scalar field $h(x)$. As in our earlier work [1, 2, 15] we will view the SSB theory (2.2) as a simplified model for the Standard Model Higgs sector in the unitary gauge.

In a generic QFT model with a massive scalar, we can define the following quantities:

1. The Feynman propagator of ϕ is the Fourier transform of the 2-point Green function,

$$\Delta(p) = \int d^4 x e^{ip \cdot x} \langle 0 | T(\phi(x) \phi(0)) | 0 \rangle = \frac{i}{p^2 - m_0^2 - \Sigma(p^2) + i\epsilon}, \quad (2.4)$$

where m_0 is the bare (unrenormalised) mass of the scalar field ϕ .

2. The self-energy $\Sigma(p^2)$ is the sum of all one-particle-irreducible (1PI) diagrams contributing to the 2-point function,

$$-i\Sigma(p^2) = \sum \text{-(1PI)} - . \quad (2.5)$$

The right-hand side of Eq. (2.4) can be interpreted in perturbation theory as the sum over the infinite series of the bare propagators and the $\Sigma(p^2)$ insertions,

$$\frac{i}{p^2 - m_0^2 - \Sigma(p^2)} = \frac{i}{p^2 - m_0^2} + \frac{i}{p^2 - m_0^2} \sum_{n=1}^{\infty} \left(-i\Sigma(p^2) \frac{i}{p^2 - m_0^2} \right)^n. \quad (2.6)$$

Hence Eq. (2.4) gives the full quantum propagator, also known as the Dyson propagator [16–18], valid in perturbative and non-perturbative quantum field theories.

3. The physical (or pole) mass m is defined as the pole of the quantum propagator (2.4),

$$m^2 - m_0^2 - \Sigma(m^2) = 0, \quad \text{or} \quad m^2 = m_0^2 + \Sigma(m^2). \quad (2.7)$$

4. The field renormalisation constant Z_ϕ is determined from the slope of $\Sigma(p^2)$ at m^2 ,

$$Z_\phi = \left(1 - \frac{d\Sigma}{dp^2} \Big|_{p^2=m^2} \right)^{-1}. \quad (2.8)$$

Using the definition of the pole mass (2.7) and the renormalisation constant Z_ϕ in (2.8), the full propagator (2.4) can be written as,

$$\Delta(p) = \frac{iZ_\phi}{p^2 - m^2 - Z_\phi[\Sigma(p^2) - \Sigma(m^2) - \Sigma'(m^2)(p^2 - m^2)]}. \quad (2.9)$$

5. The Z_ϕ constant is used to define the renormalised quantities $\Delta_R(p)$ and $\Sigma_R(p^2)$,

$$\Delta_R(p) = Z_\phi^{-1} \Delta(p), \quad (2.10)$$

$$\Sigma_R(p^2) = Z_\phi (\Sigma(p^2) - \Sigma(m^2) - \Sigma'(m^2)(p^2 - m^2)). \quad (2.11)$$

Hence, the result for the renormalised propagator in terms of all finite quantities is,

$$\Delta_R(p) = \frac{i}{p^2 - m^2 - \Sigma_R(p^2) + i\epsilon}. \quad (2.12)$$

6. The optical theorem provides the physical interpretation of the imaginary part of the self-energy in terms of the momentum-scale dependent decay width $\Gamma(p^2)$,

$$- \text{Im } \Sigma_R(p^2) = m \Gamma(p^2), \quad (2.13)$$

with the decay width being determined by the partial widths of n -particle decays at energies $s \geq (nm)^2$,

$$\Gamma(s) = \sum_{n=2}^{\infty} \Gamma_n(s), \quad \Gamma_n(s) = \frac{1}{2m} \int \frac{d\Phi_n}{n!} |\mathcal{M}(1 \rightarrow n)|^2. \quad (2.14)$$

Here \mathcal{M} is the amplitude for the $1^* \rightarrow n$ process, the integral is over the n -particle Lorentz-invariant phase space, and $1/n!$ is the Bose-Einstein symmetry factor for n spin-zero particles produced in the final state.

7. The origin of Higgslosion [1] is that the scattering amplitudes $\mathcal{M}(1 \rightarrow n)$, and consequently the decay rates into the n -particle final states, grow factorially with n in the large- n limit, $\frac{1}{n!} |\mathcal{M}_n|^2 \sim n! \lambda^n \sim e^{n \log(\lambda n)}$. When n scales linearly with the available energy, $n \sim \sqrt{s}/m$, this translates into the exponential dependence of the decay rate $\Gamma(s)$ on \sqrt{s} . It was further argued in [1, 15] that there is a sharp transition between the exponential suppression, $\Gamma_n(s < E_*^2)/m \ll 1$, and the exponential growth, $\Gamma_n(s > E_*^2)/m \gg 1$, for the n -particle rate at a certain characteristic energy scale E_* (and in a large- n limit that is still allowed by kinematics, $n \lesssim \sqrt{s}/m$). Hence in a Higgsploding theory, the propagator,

$$\Delta_R(p) = \frac{i}{p^2 - m^2 - \text{Re } \Sigma_R(p^2) + i m \Gamma(p^2) + i\epsilon}, \quad (2.15)$$

is effectively cut off at $p^2 \geq E_*^2$ by the exploding width $\Gamma(p^2)$ of the propagating state into the high-multiplicity final states. This is the *Higgspersion* effect first identified and studied in Refs. [1, 2], which is the direct consequence of Higgslosion; and it will play a central role in our discussion of quantum effects in section 3. Its physical interpretation is that the incoming highly virtual state decays rapidly into the multi-particle state made out of soft quanta with momenta $k_i^2 \sim m^2 \ll E_*^2$. The width of the propagating degree of freedom becomes much greater than its mass and the virtuality: it is no longer a simple particle state. In this sense, it has become a composite state made out of the n soft particle quanta of the same field ϕ .

The main purpose of the summary above is to demonstrate that there are no apparent subtleties that arise when accounting for the UV-renormalisation effects in the expression for the renormalised propagator (2.15). This expression is general and its validity is not restricted to, for example, the narrow width approximation.

Although we do not have much to say at present about the real part of the self-energy at $p^2 \gg m^2$ (in the regime of interest where $n \gg 1$), it is sufficient for our purposes to consider only the imaginary part, which is determined by the multi-particle decay rate $\Gamma_n(p^2)$. As soon as $\text{Im } \Sigma(p^2) = -m \Gamma_n(p^2)$ becomes exponentially large, which occurs at E_* , the propagators develop sharp exponential form-factors and vanish, thus providing a cut-off above E_* for the integrals over loop momenta. Potential cancellations between the imaginary and real parts are impossible. Essentially, it is sufficient to have the Higgsplosion of the absolute value $|\Sigma(p^2)|^2 = (\text{Re } \Sigma(p^2))^2 + (\text{Im } \Sigma(p^2))^2$.

For a more detailed introduction to Higgsplosion and some of its applications we refer the reader to Refs. [1, 2, 15] and [11, 19] and references therein. In particular, we mention here that Higgsplosion solves the fine-tuning problem of the Higgs mass by removing quantum contributions to m_0^2 from all states with masses or momenta greater than the Higgsplosion scale E_* as explained in [1]. We also note the observation of [2] that no UV divergences remain in the theory above the Higgsplosion scale E_* . The running couplings become flat above E_* and thus flow to UV fixed points, rendering the theory with Higgsplosion asymptotically safe.

2.2 Continuation to Euclidean space

In practice, all perturbative calculations in a theory, independently of whether or not it is in the Higgsplosion regime, are carried out in Euclidean space. In this paper, we rely on the conjecture that it is valid to analytically continue Higgsplosion into the Euclidean domain. In the absence of Higgsplosion, the use of the Euclidean signature $p^2 = p_0^2 + \vec{p}^2$ facilitates the UV regularisation of divergent integrals over loop momenta.¹ The analytic continuation of the momentum variable is achieved with the standard Wick rotation, $p_E^0 = ip_0$ with $\vec{p}_E = \vec{p}$, so that the propagator (2.12) becomes,

$$\Delta_R(p) = \frac{-i}{p^2 + m^2 + \Sigma_R(p^2)}. \quad (2.16)$$

In the coordinate representation, using the imaginary time,

$$\tau = it, \quad (2.17)$$

the Dyson propagator reads,

$$\Delta_R(x_1, x_2) = \langle 0 | \phi(x_1) \phi(x_2) | 0 \rangle = \int \frac{d^4 p}{(2\pi)^4} \frac{1}{p^2 + m^2 + \Sigma_R(p^2)} e^{ip_0 \Delta\tau + i\vec{p} \Delta\vec{x}}. \quad (2.18)$$

¹Dimensional regularisation, cut-off regularisation and even Pauli-Villars regularisation all are defined and normally carried out in the Euclidean signature.

When the theory enters the Higgslosion regime [1], the self-energy undergoes a sharp exponential growth. This behaviour,

$$\Sigma_R(p^2) \sim \begin{cases} 0 & : \text{for } p^2 < E_*^2 \\ \infty & : \text{for } p^2 \geq E_*^2 \end{cases}, \quad (2.19)$$

is captured by restricting the integration domain over the loop momenta. As a result, the integral over the 4-momentum in (2.16) becomes cut off by Σ outside the ball of radius E_* ,

$$\Delta_R(x_1, x_2) = \int_{p^2 \leq E_*^2} \frac{d^4 p}{(2\pi)^4} \frac{1}{p^2 + m^2} e^{ip_0 \Delta\tau + i\vec{p} \Delta\vec{x}}. \quad (2.20)$$

For non-vanishing $|\Delta x| > 0$ this integral is regular and can be straightforwardly evaluated. This leads to short-distance behaviour of the propagator of the form,

$$\Delta_R(x, 0) \sim \begin{cases} 1/|\Delta x|^2 & : \text{for } 1/E_* \ll |\Delta x| \ll 1/m \\ E_*^2 & : \text{for } |\Delta x| \lesssim 1/E_* \end{cases}. \quad (2.21)$$

This result is in agreement with Eq. (1.1). It is also clear that the absence of the singularity at $|x|^2 \rightarrow 0$ is a consequence of the dynamic integration cut-off for momenta $p^2 > E_*^2$ (i.e. above the Higgslosion scale of the self-energy).

At the same time, in the opposite limit where the point splitting Δx goes to zero, we recover from Eq. (2.20) the loop integral corresponding to the tadpole diagram,

$$\Delta_R(x, x) = \int_{p^2 \leq E_*^2} \frac{d^4 p}{(2\pi)^4} \frac{1}{p^2 + m^2}. \quad (2.22)$$

It follows that the appearance of the Higgslosion scale E_* renders this loop integral finite. In the absence of Higgslosion, the closed loop integral is quadratically divergent in the UV, as expected, and requires UV regularisation either by imposing a UV cut-off Λ_{UV} , or via dimensional or other type of UV regularisation. This is an example of the general result that Higgsploding theories are UV-finite [1, 2].

It should be noted that even in the limit of infinite E_* or Λ_{UV} , the integral in Eq. (2.20) is finite for a non-vanishing end point separation. It is regulated instead by the inverse separation $1/(\Delta t)^2$ or $1/(\Delta \vec{x})^2$. Of course, to obtain a closed loop, we will ultimately have to send this separation to zero.

2.3 Multi-particle decay width

In the preceding section we explained that the theory enters the Higgslosion phase if the decay rate of a highly virtual / highly energetic single particle state into multi-particle final states becomes exponentially large. To compute this decay rate $\Gamma_n(s)$, we need to find the amplitudes for the $1^* \rightarrow n$ processes at energies \sqrt{s} and integrate them over the n -particle phase space, as in Eq. (2.14).

We are interested in keeping the number of particles n in the final state as large as possible, that is, near the maximum number allowed by the phase space, $n \lesssim n_{\max} = \sqrt{s}/M_h$. We can therefore take the bosons in the final state to be non-relativistic. Such n -point amplitudes were studied in detail in scalar QFT in Refs. [5–8, 20], with the result,

$$\text{Model (2.1)} : \quad \mathcal{A}_{1^* \rightarrow n}(p_1 \dots p_n) = n! \left(\frac{\lambda}{8m^2} \right)^{\frac{n-1}{2}} \exp \left[-\frac{5}{6} n \varepsilon \right], \quad (2.23)$$

$$\text{Model (2.2)} : \quad \mathcal{A}_{1^* \rightarrow n}(p_1 \dots p_n) = n! \left(\frac{1}{2v} \right)^{n-1} \exp \left[-\frac{7}{6} n \varepsilon \right], \quad (2.24)$$

$$n \rightarrow \infty, \quad \varepsilon \rightarrow 0, \quad n \varepsilon = \text{fixed}.$$

As indicated, these tree-level amplitudes are computed in the double-scaling limit with large multiplicities $n \gg 1$ and small non-relativistic energies of each individual particle, $\varepsilon \ll 1$, where,

$$\varepsilon = \frac{\sqrt{s} - nm}{nm} = \frac{1}{nm} E_n^{\text{kin}} \simeq \frac{1}{n} \frac{1}{2m^2} \sum_{i=1}^n \vec{p}_i^2, \quad (2.25)$$

so that the total kinetic energy per particle mass $n \varepsilon$ in the final state is fixed.

The pre-exponential factors on the right-hand side of Eqs. (2.23)-(2.24) correspond to the tree-level amplitudes (or more precisely, currents with one incoming off-shell leg) computed on the n -particle thresholds. In the elegant formalism of Brown [5], these amplitudes for all n arise from the generating functional ϕ_0 , which is given by a spatially-uniform solution to the classical equations of motion.² These solutions are easily found by solving the classical equations of motion corresponding to models (2.1)-(2.2), and read,

$$\text{Model (2.1)} : \quad \phi_0(t) = \frac{z(t)}{1 - \lambda z(t)^2/(8m^2)}, \quad \text{where} \quad z = z_0 e^{imt} \quad (2.26)$$

$$\text{Model (2.2)} : \quad \phi_0(t) = v \left(\frac{1 + z(t)/(2v)}{1 + z(t)/(2v)} \right), \quad \text{where} \quad z = z_0 e^{im_h t} \quad (2.27)$$

Then the amplitudes on n -particle mass thresholds are given by differentiating these classical generating functions n times with respect to the source variable z ,

$$\mathcal{A}_{\text{tree } 1^* \rightarrow n}^{\text{thr.}} := \langle n | \phi | 0 \rangle_{\text{tree}} = \left(\frac{\partial}{\partial z} \right)^n \phi_0(z) |_{z=0} = \begin{cases} n! \left(\frac{\lambda}{8m^2} \right)^{\frac{n-1}{2}} \\ n! \left(\frac{1}{2v} \right)^{n-1} = n! \left(\frac{\lambda}{m_h^2} \right)^{\frac{n-1}{2}}. \end{cases} \quad (2.28)$$

These are exact expressions for tree-level amplitudes valid for any value of n [5].

The amplitudes in Eqs. (2.23)-(2.24) go beyond the threshold results (2.28) by accounting for the kinematic dependence in the non-relativistic limit of the external momenta. These were derived as a non-relativistic deformation of the Brown's generating functions method in Refs. [8] and [20] for the unbroken and the broken theories respectively. The amplitudes now contain an exponential form-factor that depends on the kinetic energy of

²Tree level is equivalent to the leading-order expansion in \hbar , thus reducing the quantum problem to classical solutions. Furthermore, the vanishing external 3-momenta of the on-the-threshold amplitudes selects spatially-uniform time-dependent solutions [5].

the final state $n\varepsilon$. But, importantly, the factorial growth $\sim \lambda^{n/2} n!$ characteristic to the multi-particle amplitude on mass threshold remains. Its occurrence can be traced back to the factorially growing number of Feynman diagrams at large n and the lack of destructive interference between the diagrams in the scalar theory. In Section 3 we will compute the leading-order quantum corrections to these tree-level amplitudes, in the case where a non-trivial finite Higgs explosion scale E_* is present.

To obtain the self-energy, $\text{Im } \Sigma_R(p^2) = -m \Gamma(p^2)$, we integrate the amplitudes³ (2.23)-(2.24) over the n -particle phase-space for large n ,

$$\Gamma_n(s) = \frac{1}{2m} \int \frac{d\Phi_n}{n!} |\mathcal{M}_{1 \rightarrow n}|^2. \quad (2.29)$$

For the unbroken theory (2.1), one finds [12, 13],

$$\Gamma_n(s) \propto \mathcal{R}(\lambda; n, \varepsilon) = \exp \left[n \left(\log \frac{\lambda n}{16} + \frac{3}{2} \log \frac{\varepsilon}{3\pi} + \frac{1}{2} - \frac{17}{12} \varepsilon + Q(\lambda n, \varepsilon) \right) \right], \quad (2.30)$$

and for the model with SSB (2.2) [20],

$$\Gamma_n(s) \propto \mathcal{R}(\lambda; n, \varepsilon) = \exp \left[n \left(\log \frac{\lambda n}{4} + \frac{3}{2} \log \frac{\varepsilon}{3\pi} + \frac{1}{2} - \frac{25}{12} \varepsilon + Q(\lambda n, \varepsilon) \right) \right]. \quad (2.31)$$

In particular, note that the ubiquitous factorial growth of the large- n amplitudes translates into the $\frac{1}{n!} |\mathcal{M}_n|^2 \sim n! \lambda^n \sim e^{n \log(\lambda n)}$ factor in the rates \mathcal{R} above. The term $Q(\lambda n, \varepsilon)$ on the right-hand side of both equations above indicates quantum corrections: at tree level $Q(\lambda n, \varepsilon) \equiv 0$.

These rates can also be computed using an alternative semi-classical method formulated by Son in Ref. [12]. This is an intrinsically non-perturbative approach, with no reference in its outset made to perturbation theory. The path integrals contributing to the amplitudes and the rates are computed in the steepest descent method, controlled by two large parameters, $1/\lambda \rightarrow \infty$ and $n \rightarrow \infty$. More precisely, the limit is,

$$\lambda \rightarrow 0, \quad n \rightarrow \infty, \quad \text{with} \quad \lambda n = \text{fixed}, \quad \varepsilon = \text{fixed}. \quad (2.32)$$

The semi-classical computation carried out in [12], in the regime where,

$$\lambda n = \text{fixed} \ll 1, \quad \varepsilon = \text{fixed} \ll 1, \quad (2.33)$$

provided an alternative derivation of the tree-level perturbative results for non-relativistic final states (2.30)-(2.31), with the expressions being correctly reproduced. Remarkably, this semi-classical calculation also reproduces the leading-order quantum corrections arising from resumming one-loop effects. These were previously computed perturbatively in the $\varepsilon \rightarrow 0$ limit in [8–10],

$$Q_{1\text{-loop}}(\lambda n) = \begin{cases} -\lambda n \text{ Re } F/8 & : \text{Model (2.1)} \\ +\lambda n \text{ } 2B & : \text{Model (2.2)} \end{cases}, \quad (2.34)$$

³Note that the conventionally-normalised amplitudes $\mathcal{M}_{1^* \rightarrow n}$ are obtained from the currents $\mathcal{A}_{1^* \rightarrow n}$ in (2.23)-(2.24) by the LSZ amputation of the single off-shell incoming line, $\mathcal{M}_{1 \rightarrow n} := (s - M_h^2) \cdot \mathcal{A}_{1^* \rightarrow n}(p_1 \dots p_n)$.

where the constant coefficients F and B will be given in Eqs. (3.30) and (3.49) below. This agreement constitutes an important test of the applicability of the semi-classical method of Son for computations of quantum corrections. In Section 3 we will verify that this agreement persists when the perturbative loop integrals are carried out in the presence of the Higgslosion scale E_* .

The semi-classical approach is equally applicable and more relevant to the realisation of the non-perturbative Higgslosion case where,

$$\lambda n = \text{fixed} \gg 1, \quad \varepsilon = \text{fixed} \ll 1. \quad (2.35)$$

This calculation was carried out in Ref. [15] for the spontaneously broken theory (2.2), with the result given by,

$$\mathcal{R}_n(\lambda; n, \varepsilon) = \exp \left[\frac{\lambda n}{\lambda} \left(\log \frac{\lambda n}{4} + 0.85 \sqrt{\lambda n} + \frac{1}{2} + \frac{3}{2} \log \frac{\varepsilon}{3\pi} - \frac{25}{12} \varepsilon \right) \right], \quad (2.36)$$

which is equivalent to Eq. (2.31) with the substitution,

$$Q_{\lambda n \gg 1}(\lambda n) = +0.85 \sqrt{\lambda n}. \quad (2.37)$$

This result (2.37) [15] also agrees with an earlier calculation of the semi-classical amplitude on threshold in Ref. [14].

Higgslosion becomes operative when the decay width, or equivalently the rate (2.36), becomes exponentially large. Let us estimate the energy E_* where this occurs. The expression (2.36) was derived in the near-threshold limit (2.35), where the parameter ε is treated as a fixed constant much smaller than one. The initial state energy and the final state multiplicity are related linearly via $E/m_h = (1+\varepsilon)n$. Hence, for any fixed ε , one can raise the energy to obtain an arbitrarily large n , and consequently, a large $\sqrt{\lambda n}$. The negative $\log \varepsilon$ term and the positive $\sqrt{\lambda n}$ term in (2.36) are in competition. Nonetheless, there is always a range of sufficiently high multiplicities, where $\sqrt{\lambda n}$ overtakes the logarithmic term $\log \varepsilon$ for any fixed (however small) value of ε . This leads to the exponentially growing multi-particle rates. It was shown in Ref. [1] that in the model where the multi-particle rates are given by the expression (2.36), and fixing $\lambda = 1/8$, the rates start growing exponentially when $E_* \sim 200m_h$.

2.4 Where is Higgspersion in the semi-classical calculation?

To compute the n -particle decay width $\Gamma_n(E)$ in Eq. (2.29) one starts with the amplitude $\mathcal{M}_{1 \rightarrow n}$ between an off-shell single particle state and an n -particle on-shell final state. The amplitude itself is obtained from the n -particle form factors of generic local operators $\mathcal{O}(x)$ in the theory. The form factors are defined as matrix elements of the operator $\mathcal{O}(x)$ at the origin, $x = 0$, between the vacuum in-state and the n -particle out-state $|n\rangle_E^{\text{out}}$ of the fixed total energy E (or more precisely $p_{\text{fin}}^2 = E^2$),

$$F_{\mathcal{O}}(n; E) = {}^{\text{in}}\langle 0 | \mathcal{O}(0) | n \rangle_E^{\text{out}}. \quad (2.38)$$

The local operator $\mathcal{O}(0)$ creates an off-shell state at the spacetime point $x = 0$ from the in-state vacuum. The virtuality of this state is $p^2 = E^2$ which is guaranteed by the energy conservation in the transition process to the final state.

The $1^* \rightarrow n$ amplitude of interest is obtained from the form factor (2.38) for the operator $\mathcal{O}(x) = \phi(x)$ by LSZ amputating the single incoming ϕ -leg,

$$(\text{LSZ})_\phi^1 \cdot F_\phi(n; E), \quad \text{where} \quad F_\phi(n; E) = {}^{\text{in}}\langle 0 | \phi(0) | n \rangle_E^{\text{out}}. \quad (2.39)$$

On the other hand, as was explained in [12], the semi-classical formalism for computing the n -particle rates cannot be used when the operator is the elementary field, $\mathcal{O}(x) = \phi(x)$. Instead the formalism was developed in [12] for the case when the initial off-shell state was created by a composite local operator. The operator used in [12] was an exponential, $\mathcal{O}(x) = e^{j\phi(x)}$, so that one can obtain the semi-classical approximation for the n -particle rates of the type,

$$\mathcal{R}_n(E) = \lim_{j \rightarrow 0} \int \frac{d\Phi_n}{n!} \left| {}^{\text{in}}\langle 0 | e^{j\phi(0)} | n \rangle_E^{\text{out}} \right|^2 = \lim_{j \rightarrow 0} \int \frac{d\Phi_n}{n!} |F_{\mathcal{O}}(n; E)|^2. \quad (2.40)$$

The semi-classical approximation to (2.40) is the expression in Eq. (2.36) derived in [15] and valid in the large- n regime (2.35).

There are two questions we would like to comment on: 1) How does the semi-classical computation of the ‘wrong’ observable $\propto |F_{\mathcal{O}}(n; E)|^2$ relate to the original observable $\propto |F_\phi(n; E)|^2$, which corresponds to the transitioning of the ‘physical’ 1-particle state to n final-state particles? 2) How does Higgspersion impact on the semi-classical rate (2.40) and (2.36)?

To answer the first question we quote [12] in stating that the current semi-classical approximation can be trusted only to an exponential accuracy, and the dependence of the final result on the specific form of the operators $\mathcal{O}(x)$ used in the calculation affects only the factor in front of the exponent in (2.36). Essentially, this statement is a conjecture of the underlying approach [12, 21] — it was partially evidenced in Ref. [22] but still remains a conjecture. We do not have a new insight on this quite well-known technical problem, and will assume that the semi-classical computation of the rate in (2.40) does give correct information about the exponential form of the physical rate.

There is however an important point relevant for this conjecture of Son and others that we want to emphasise. As we shall explain now, the semi-classical equivalence between observables made out of the operators $\mathcal{O}(x)$ and the operators $\phi(x)$ is between the *decay rates* of the appropriate initial states into n -particle states, not between the form factors of $\mathcal{O}(x)$ and $\phi(x)$ themselves. The definition of the decay rate involves matrix elements where all external propagators have been LSZ-amputated, so in particular, the initial state is non-propagating. Hence the semi-classical equivalence is between,

$$(\text{LSZ})_\phi^1 \cdot {}^{\text{in}}\langle 0 | \phi(0) | n \rangle_E^{\text{out}} \quad \text{and} \quad {}^{\text{in}}\langle 0 | \mathcal{O}(0) | n \rangle_E^{\text{out}}, \quad (2.41)$$

where the factor $(\text{LSZ})_\phi^1$ implies the LSZ amputation of the external propagator of the in-state ${}^{\text{in}}\langle 0 | \phi(0)$. At the same time, there is no such factor on the right-hand side since, as we will see momentarily, the state ${}^{\text{in}}\langle 0 | \mathcal{O}(0)$ is already LSZ-reduced.

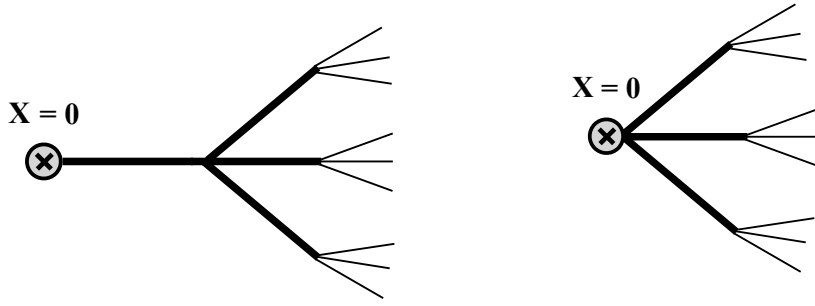


Figure 1: The form factor $F_\phi(n; E)$ of the elementary field $\phi(0)$ is shown in the left diagram, versus the form factor $F_\mathcal{O}(n; E)$ of the composite local operator $\mathcal{O}(0) = \phi^3(0)$, depicted on the right. Thick lines denote full propagators, thin lines indicate the on-shell n -particle final state (in this case $n = 9$) with the corresponding propagators already removed.

One way to see this is to imagine extending the theory by adding a source term to its Lagrangian and a kinetic term for the new degree of freedom,

$$\int d^4x \mathcal{L}[\phi(x)] + \int d^4x s(x) \mathcal{O}(x) - \int d^4x s(x) \mathcal{K} s(x). \quad (2.42)$$

Here $s(x)$ is a field describing a new degree of freedom, $\mathcal{O}(x)$ — a composite operator made out of ϕ — is its source coupled to the field $s(x)$, and \mathcal{K} is the kinetic operator acting on s , i.e. the inverse s -propagator, $\partial_\mu \partial^\mu + M_s^2$.

The matrix elements to be compared are,

$${}^{\text{in}}\langle 0|\phi(0)|n\rangle_E^{\text{out}} \quad \text{and} \quad {}^{\text{in}}\langle 0|s(0)|n\rangle_E^{\text{out}}, \quad (2.43)$$

both containing the incoming propagator for the initial state created by either ϕ or s from the vacuum. After LSZ-reducing the incoming propagator in each case, we obtain

$$(\text{LSZ})_\phi^1 \cdot {}^{\text{in}}\langle 0|\phi(0)|n\rangle_E^{\text{out}} \quad \text{and} \quad (\text{LSZ})_s^1 \cdot {}^{\text{in}}\langle 0|s(0)|n\rangle_E^{\text{out}} = {}^{\text{in}}\langle 0|\mathcal{O}(0)|n\rangle_E^{\text{out}}. \quad (2.44)$$

$\mathcal{O}(x)$ is the source term of the field $s(x)$, i.e. $\mathcal{K} \cdot s(x) = \mathcal{O}(x)$, and it no longer contains the incoming propagator which has been LSZ-amputated. (We note that the role of the composite operator $\mathcal{O}(x)$ as the source \mathcal{J} for a new degree of freedom $s(x)$ and the appearance of $\mathcal{O}(x)$ in the LSZ-amputated amplitudes is completely analogous to the Witten diagrams [23] in the context of the AdS/CFT correspondence.) Eq. (2.41) follows from this observation. The decay rates computed from these two matrix elements are supposed to be equivalent within the semi-classical approximation of [12] but we note that we are comparing the pure form factor of the composite operator ${}^{\text{in}}\langle 0|\mathcal{O}(0)|n\rangle_E^{\text{out}}$ to the form factor $(\text{LSZ})_\phi^1 \cdot {}^{\text{in}}\langle 0|\phi(0)|n\rangle_E^{\text{out}}$ acted on by the LSZ operator. Without the LSZ reduction, the form factor of the elementary field ${}^{\text{in}}\langle 0|\phi(0)|n\rangle_E^{\text{out}}$ would be suppressed by the effect of the self-energy in the external propagator — the Higgspersion effect [1].

We can also see this difference between the form factors for the elementary field operator $\phi(x)$ and for the local composite operators $\mathcal{O}(x)$ diagrammatically. A Feynman

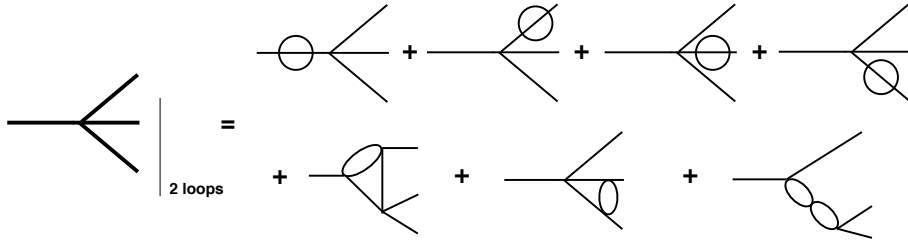


Figure 2: The form factor $F_\phi(n; E)$ of the elementary field $\phi(0)$ at 2-loop order.

diagram representation of the form factor $F_\phi(n; E)$ in (2.39) is shown on the left diagram in Fig. 1. We note that this form factor contains the propagator connecting the point $x = 0$ where the fundamental field operator $\phi(0)$ is located, to the first interaction vertex. The propagator is the full propagator (2.15) of the interacting theory,

$$\Delta(p) = \frac{i}{p^2 - m^2 - \Sigma(p^2) + i\epsilon}, \quad (2.45)$$

and since it includes the self-energy contribution, it automatically accounts for the effect of Higgspersion at the momentum scale where $\Sigma(p^2) \gtrsim p^2$. On the other hand, diagrams for *composite local* operators $\mathcal{O}(x)$ do not have an incoming propagator. It is easily seen from the right diagram in Fig. 1 which corresponds to $\mathcal{O}(0) = \phi^3(0)$ (but can equally well be used for any composite operator $\mathcal{O}(0) = \phi^n(0)$) that the point $x = 0$ is the vertex, rather than the end point of the in-state propagator associated with $\phi(0)$. Thus, the form factors of composite operators used in the semi-classical calculation do not include the Higgspersion effect as there is no in-state propagator, while the form factor of the elementary field does account for Higgspersion.

One can perhaps better visualise the difference between the form factors in Fig. 1 by considering the 2-loop perturbative contribution to the form factor of the elementary field ϕ . It is shown in Fig. 2 for the ϕ^4 theory. Clearly, there are self-energy corrections to the incoming propagator (shown in the first diagram on the right-hand side) thus resulting in this propagator becoming of the form (2.45) after the resummation. On the other hand, there are no such contributions for the form factors of composite operators, such as shown in the diagram on the right of Fig. 1. Of course one can draw some one-particle-reducible diagrams contributing to the form factors of composite operators, such as the ones shown in Fig. 3, but it is easy to see that at energies $\sqrt{s} \sim E_*$ their contributions are negligible relative to those on the right diagram in Fig. 1. The reason is that the diagrams in Fig. 3 are exponentially suppressed by Higgspersion in the single intermediate propagator at $p^2 = s \gtrsim E_*^2$, while the diagrams on the right plot in Fig. 1 are not. In the latter case the dominant contributions come from the energies and momenta split roughly in 3, hence the virtuality scale in each of the three branches would be $\sim E_*/3$ which makes the Higgspersion effect completely negligible. Similar considerations were explored in more detail in an earlier publication [2].

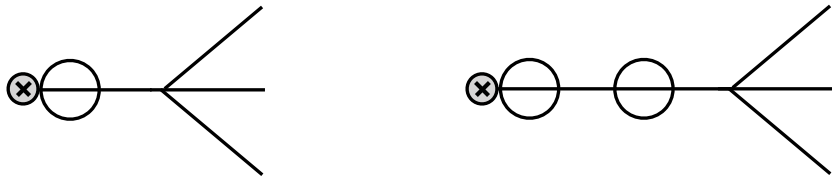


Figure 3: Contributions to the form factor $F_{\phi^3}(n; E)$ suppressed by Higgspersion due to the appearance of the single intermediate propagator. For more details see also [2].

Of course, as we have already explained, for the calculation of the actual decay rates Γ_n , in each case one needs to start from the matrix elements with the LSZ-reduced external lines. In other words, the incoming line for the form factor on the left figure in Fig. 1 should be LSZ amputated in accordance with (2.39), while the form factor of the composite operator on the right diagram in Fig. 1 is already without the external propagator. Thus, the actual decay rate $\Gamma_n(E) \propto \mathcal{R}_n(E)$ does not contain the Higgspersing propagator for the in-state in either case. As the semi-classical calculation in [12, 15] was based on form factors of composite operators, it did not require an additional LSZ amputation of the incoming full propagator as it was not there in the first place. The rate in (2.40) is the imaginary part of the self-energy $\Sigma(p^2)$ in (2.45); it is not the imaginary part of the whole propagator (2.45).

If it was possible to directly compute the form factors of the fundamental operators $F_\phi(n; E)$ in some alternative formalism, rather than working with the composite operator form factors $F_O(n; E)$, one would then have to LSZ amputate the external propagators from the integral,

$$(\text{LSZ})_\phi^2 \cdot \int \frac{d\Phi_n}{n!} |F_\phi(n; E)|^2 , \quad (2.46)$$

as an additional step, but as we have explained above, this is not needed for our composite operator-based WKB derivation.

It is only when we want to consider a physical scattering process of 2 to n particles that we need to restore the propagator (2.45) of the off-shell state 1^* . Hence, we conclude that the fully LSZ-amputated decay rates Γ_n can Higgsplode, but the physical scattering processes will always include the Higgspersing propagator and will be well behaved at high energies and consistent with unitarity.

2.5 The Higgsplosion scale E_*

In general, the Higgsplosion scale E_* is defined as the new dynamically generated scale of the weakly coupled theory, $\lambda \ll 1$, where a sharp transition occurs between the negligibly small multi-particle rates at $E < E_*$, and the exponentially large rates at $E > E_*$. From general principles, it is clear that this scale would have the parametric dependence of the

form,

$$E_* = \frac{m_h}{f(\lambda)} , \quad \text{where } f(\lambda)|_{\lambda \rightarrow 0} \rightarrow 0 . \quad (2.47)$$

The mass m_h is the only dimensionful parameter of the theory and the fact that E_* goes to infinity in the free-theory limit $\lambda \rightarrow 0$ is also obvious since in this limit no multi-boson production is possible. Hence, the singularity at $\lambda = 0$ implies that the Higgslosion scale is non-perturbative.

To sharpen this argument for the emergence of E_* (as the new dynamical scale in a weakly coupled theory with microscopic massive scalars), we would like to get a better handle on $f(\lambda)$ in the context of the model with spontaneously broken symmetry (2.2). The rate, in this case, is given in Eq. (2.36). It will be useful to introduce the more natural rescaled variables for the multi-particle rate \mathcal{R} ,

$$\tilde{n} = \lambda n , \quad \tilde{E} = \frac{\lambda E}{m_h} , \quad (2.48)$$

so that

$$\tilde{E} = (1 + \varepsilon) \tilde{n} . \quad (2.49)$$

Following closely the discussion in Section 5 of Ref. [15], we now re-write the expression for the rate in the following form,

$$\mathcal{R}_n(E) \sim \int_0^{\varepsilon_{nr}} d\varepsilon \left(\frac{\varepsilon}{3\pi} \right)^{\frac{3n}{2}} \exp \left[\frac{\tilde{n}}{\lambda} \left(0.85 \sqrt{\tilde{n}} + \log \tilde{n} - a\varepsilon \tilde{n}^p - \text{const} \right) \right] . \quad (2.50)$$

The integral $\int_0^{\varepsilon_{nr}} d\varepsilon \left(\frac{\varepsilon}{3\pi} \right)^{\frac{3n}{2}}$ appearing on the right-hand side is nothing but the non-relativistic phase-space integral $\int d\Phi_n$ written in the large- n limit. The upper limit of the integration, ε_{nr} , is the non-relativistic kinetic energy per particle per mass, $\varepsilon_{nr} = E/(nm_h) - 1 \ll 1$ while ε is now treated on the right-hand side of (2.50) as the integration variable.

The second point to note is that we introduced an additional term, $-a\varepsilon \tilde{n}^p$, in the exponent on the right-hand side of (2.50) which represents the sub-leading correction in $\varepsilon \ll 1$ to the expression in (2.37). In other words, we have assumed that,

$$Q_{\tilde{n} \gg 1}(\tilde{n}, \varepsilon) = +0.85 \sqrt{\tilde{n}} - a\varepsilon \tilde{n}^p + \text{higher orders in } \varepsilon , \quad (2.51)$$

where a and p are some positive constants. The integral we have to compute is,

$$\mathcal{R}_n \sim e^{\frac{\tilde{n}}{\lambda} (0.85 \sqrt{\tilde{n}} + \log \tilde{n} - \tilde{c})} \int d\varepsilon e^{\frac{\tilde{n}}{\lambda} \left(\frac{3}{2} \log \varepsilon - a\varepsilon \tilde{n}^p \right)} , \quad (2.52)$$

where

$$\tilde{c} = \log 4 + \frac{3}{2} \log 3\pi - \frac{1}{2} . \quad (2.53)$$

The saddle-point dominating the integral over ε is,

$$\varepsilon_* = \frac{3}{2} \frac{1}{a} \frac{1}{\tilde{n}^p} , \quad (2.54)$$

and the value of the original integral for $\mathcal{R}_n(\varepsilon)$ at the saddle-point is,

$$\mathcal{R}_n(\varepsilon_\star) \sim \exp \left[\frac{\tilde{n}}{\lambda} \left(0.85 \sqrt{\tilde{n}} + \left(1 - \frac{3p}{2} \right) \log \tilde{n} - \text{const}' \right) \right]. \quad (2.55)$$

The constant term const' is,

$$\text{const}' = \tilde{c} + \frac{3}{2} \left(1 - \log \frac{3}{2a} \right) = 1 + \log 4 + \frac{3}{2} \log 2a\pi. \quad (2.56)$$

Setting $a = 1$, we have $\text{const}' \simeq 5.14$.

Now, assuming that the coefficient in front of the logarithmic term in ε in (2.55) is positive, i.e. $0 < p < 2/3$, the exponent is negative at small \tilde{n} , positive at large \tilde{n} and crosses zero at some value \tilde{n}_* . For example, for $p = 1/2$ and $a = 1$, which corresponds to the NLO correction $-a\varepsilon\tilde{n}^p = -\varepsilon\sqrt{\tilde{n}}$, the value of $\tilde{n}_* \simeq 5.55$.

In the alternative scenario, where the coefficient in front of the logarithm is negative, for example at $p = 1$, the function in the exponent of (2.55) has a more complicated behaviour with a local minimum at intermediate values of \tilde{n} . Nevertheless at larger \tilde{n} , the function is again monotonic and crosses over from negative to positive values at $\tilde{n}_* \simeq 7.2$.

It then follows that the value of $\tilde{E}_* = (1 + \varepsilon_\star) n_* \simeq \tilde{n}_* := C = \text{const}$. As a result, we can write the Higgslosion scale E_* as,

$$E_* = C \frac{m_h}{\lambda}. \quad (2.57)$$

It is also easy to verify that this conclusion is consistent within the validity of the non-relativistic limit.

The parametric dependence of the Higgslosion energy E_* on the particle mass and the inverse coupling constant is reminiscent of another famous dynamically induced scale in the electroweak theory — the mass of the sphaleron solution [3, 4], $M_{\text{sph}} = \text{const} \frac{m_W}{\alpha_w}$. Both scales are non-perturbative and semi-classical in nature. They do not appear in the Lagrangian of the theory, but rather characterise the energy scale where the transition to novel dynamics involving multi-particle states occurs.⁴ The sphaleron, however, does not occur in the pure scalar sector of the theory and requires the $SU(2)$ gauge theory in the Higgs phase.

2.6 Comment on the possibility of non-analytic corrections in ε to the large- n WKB amplitudes

Before closing this section, we would like to consider the possibility that our semi-classical rate $\mathcal{R}_n(E)$ could also contain non-analytic corrections in ε in the near-threshold kinematics $\varepsilon \rightarrow 0$.

The discussion in Ref. [15], and the resulting realisation of Higgslosion, was based on the simplifying assumption that the currently unknown higher-order corrections to the

⁴In the case of sphalerons, the new dynamics is that of the non-perturbative $(B+L)$ -violating transitions between multi-particle initial and final states.

$1^* \rightarrow n$ amplitudes (or form factors) are analytic in the parameter ε , at $\varepsilon \sim 0$. Indeed taking the leading-order term in the Taylor expansion $\sim \varepsilon^1$ of the correction to be of the form $-a\varepsilon\tilde{n}^p$, we saw in the last section that the saddle-point value of ε was power-suppressed at $\tilde{n} = \lambda n \gg 1$, and that the rate \mathcal{R}_n at this point was exponentially large (2.50) in the large \tilde{n} limit, thus signalling Higgsplosion.

However the reader may question what would be the effect of adding to the exponent in (2.50) a *non-analytic* correction, in particular a slowly varying one, of the type $d(\tilde{n})/\log \varepsilon$. In the limit $\varepsilon \rightarrow 0$ and \tilde{n} held fixed, this correction vanishes, i.e. $d(\tilde{n})/\log \varepsilon \rightarrow 0$. Thus, it does not modify the known semi-classical expression for the amplitude on the n -particle threshold. Since the dependence on ε is now inverse logarithmic rather than power-like, this correction does affect the $0 < \varepsilon < 1$ behaviour of the rate (2.36) in the large \tilde{n} limit which now becomes,

$$\tilde{\mathcal{R}}_n(E) = \exp \left[\frac{\tilde{n}}{\lambda} \left(\frac{3}{2} \log \frac{\varepsilon}{3\pi} + 0.85 \sqrt{\tilde{n}} + \frac{d(\tilde{n})}{\log \varepsilon} + \log \tilde{n} - \text{const} \right) \right]. \quad (2.58)$$

If the coefficient function $d(\tilde{n})$ is positive and grows with \tilde{n} faster than $0.85\sqrt{\tilde{n}}$ it would result in the exponential suppression of the rate and prevent Higgsplosion from being realised.

Can such non-analytic corrections be generated in a simple quantum theory? One could ask why should all corrections to the exponent of the n -particle rate (2.36) be analytic, if the term $\sim \log \varepsilon$, that was already present in the original rate (2.36), is not.

However, we know that the existing $\sim \log \varepsilon$ term in the exponent of the rate (2.58) arises from the volume of the n -particle phase-space, and has nothing to do with the amplitudes themselves,

$$\int d\Phi_n \sim \int_0^{\varepsilon_{nr}} d\varepsilon \left(\frac{\varepsilon}{3\pi} \right)^{\frac{3n}{2}} \sim \exp \left[n \left(\frac{3}{2} \log \frac{\varepsilon}{3\pi} \right) \right]. \quad (2.59)$$

The entire logarithmic factor came from taking the logarithm of the n -particle non-relativistic phase-space. We also note that there is no dependence on the coupling constant in this factor. Thus, this particular logarithmic term is well-understood and has nothing to do with the amplitudes. On the other hand, in order to generate a term of the type $d(\tilde{n})/\log \varepsilon$, one needs an effect coming from the amplitudes directly, since it does not arise as a correction to the phase-space volume. Therefore, it has to be (twice) the leading correction in ε to the scattering amplitude on threshold.

We do not have a rigorous argument to prove that the non-analytic corrections of the form $d(\tilde{n})/\log \varepsilon$ cannot be generated in the large- λn amplitudes,

$$\mathcal{M}_{1 \rightarrow n} \stackrel{?}{=} \mathcal{M}_{1 \rightarrow n}^{\text{threshold}} \times \exp \left[-\frac{n d(\lambda n)}{2 \log 1/\varepsilon} \right]. \quad (2.60)$$

However, we can offer an intuitive reasoning against the appearance of such terms. Let us consider the amplitudes $\mathcal{M}_{1 \rightarrow n}$ near its n -particle threshold as a function of two variables, λn and ε . Since the amplitude of interest is always near the threshold, we will assume that

$\varepsilon \ll 1$ but will allow the second argument, λn , to vary freely from small to large values. In the regime where λn is small, the ordinary perturbation theory is applicable and the amplitude is of the form,

$$\frac{1}{n} \log \left(\mathcal{M}_{1 \rightarrow n} / \mathcal{M}_{1 \rightarrow n}^{\text{tree}} \right) = \sum_{p=1}^{\infty} (\lambda n)^p B_p(\varepsilon), \quad (2.61)$$

where the sum is over the loop orders in perturbation theory. The functions $B_p(\varepsilon)$ describe the kinematic dependence at each loop order, and since we are interested only in the near-threshold behaviour, we can consider their small ε expansion. We expect that in a QFT with a mass gap and in the number of dimensions not less than 4, all perturbative functions $B_p(\varepsilon)$ should be analytic in the vicinity of $\varepsilon \sim 0$, so that,

$$B_p(\varepsilon) = B_p^{(0)} + B_p^{(1)}\varepsilon + B_p^{(2)}\varepsilon^2 + \dots, \quad (2.62)$$

where the constant $B_1^{(0)}$ for the 1-loop function is equal to the constant B in (2.34). Any appearance of the non-analytic contributions to $B_p(\varepsilon)$ of the type $1/\log \varepsilon$ would imply that a derivative with respect to ε of the perturbative amplitude in (2.61) will be singular at $\varepsilon = 0$. This is equivalent to saying that a derivative with respect to an external momentum \vec{p}_i of a non-relativistic perturbative amplitude at small values of \vec{p}_i would be infinite. However the Feynman diagrams of our scalar theory with a mass gap and in the number of dimensions not less than 4, are regular and differentiable in the infrared regime of $\varepsilon \rightarrow 0$ or $p_i^2 \rightarrow 0$. Hence we will take that the behaviour (2.61) and (2.62) is justified in the regime of small λn .

The next step is to resum the perturbation theory in λn for each fixed power of ε . The intuitive expectation is that while this resummation is non-trivial, it should not generate any new functional dependence on ε that has not already been there. The formally resummed result can then be continued to the large λn limit, without generating the dangerous non-differentiable dependence on ε .

The intuitive argument presented above is not a proof and poses an interesting problem for a future study.⁵ This question of the possibility of the non-analytic and non-differentiable corrections to the amplitudes in the near-threshold limit should ultimately be settled with an explicit calculation. We expect that it should be possible to carry out such a calculation by introducing a small ε and extending the existing semi-classical analysis for the amplitudes on the multi-particle thresholds.

3 Systematics of loops with Higgspersion

3.1 Computing a loop with the propagator in the classical background

We will start by considering the scalar field theory (2.1) with unbroken Z_2 symmetry, and postpone the discussion of the broken theory (2.2) to Section 3.3. As we have already

⁵In fact, it was proposed in Ref. [14] that an additional kinematic suppression could occur non-perturbatively. In our view their effect has more to do with the unitarity restoration, i.e. Higgspersion, and is already accounted for. But the whole point certainly deserves further study.

explained, the generating functional for all tree-level amplitudes on n -particle thresholds is given in this model by the classical solution (2.26).

The aim of this section is to compute the leading-order quantum corrections to these amplitudes in the case where a non-trivial finite Higgslosion scale E_* is present. The leading order calculation (in the absence of Higgslosion) was performed in [9], extended to the spontaneously broken theory in [10], and generalised in [8] to include all higher-loop effects by exponentiation to the leading order in λn .

We begin by following closely the original leading-loop calculation of Voloshin in [9], and then explain how it should be modified to reflect the appearance of the Higgslosion scale E_* . This will allow us to assess the effect of Higgslosion on the RG running of the parameters of the theory, including their asymptotic safety. We will also see that the so-called finite terms arising from the quantum effect are the same as those computed in [8–10] up to corrections of the order $\mathcal{O}(m^2/E_*^2)$. These considerations will pave the way for computing precision observables in Higgslosion in Section 4.

The quantum corrections to the tree-level amplitudes (2.28) are obtained by expanding around the classical field, $\phi(x) = \phi_0(x) + \phi_q(x)$, so that the Euclidean Lagrangian (2.1) for the quantum fluctuation ϕ_q becomes,

$$\mathcal{L} = \frac{1}{2}(\partial_\mu \phi_q)^2 + \frac{1}{2}(m^2 + 3\lambda\phi_0^2)\phi_q^2 + \lambda\phi_0\phi_q^3 + \frac{\lambda}{4}\phi_q^4. \quad (3.1)$$

One then integrates out $\phi_q(x)$ using the background field perturbation theory.

It follows that the generating functional of the amplitudes in the full quantum theory is obtained by promoting the classical solution ϕ_0 into the quantum expectation value $\langle\phi\rangle = \phi_0 + \langle\phi_q\rangle$. Individual amplitudes are then computed via

$$\langle n|\phi|0\rangle = \left(\frac{\partial}{\partial z_0}\right)^n (\phi_0 + \langle\phi_q\rangle)|_{z_0=0}. \quad (3.2)$$

This provides the generalisation to full quantum theory [8, 9] of the tree-level formalism of Brown [5] for computing $1^* \rightarrow n$ amplitudes on n -particle mass-thresholds.

The matrix element $\langle\phi_q\rangle$ is computed using the Feynman rules following from the action (3.1). It is easy to see that the one-loop contribution to $\langle\phi_q\rangle$ comes from the tadpole diagram, which contains the three-point vertex from (3.1) with two attached propagators: one external, $G(y, x)$, and one forming the loop, $G(x, x)$,

$$\langle\phi_q(y)\rangle_{1\text{-loop}} = (-3\lambda) \int d^4x G(y, x) \phi_0(x) G(x, x), \quad (3.3)$$

where $G(x_1, x_2)$ is the propagator for the scalar field ϕ_q in the background of the classical solution,⁶

$$G(x_1, x_2) = \langle 0|\phi_q(x_1)\phi_q(x_2)|0\rangle, \quad (3.4)$$

⁶To distinguish the propagator in the background of $\phi_0(t)$ from the propagator in the trivial background, we call it G rather than Δ . We also continue working in Euclidean space and thus drop the T -ordering in the propagator.

which satisfies the equation,

$$\left(-\left(\frac{\partial}{\partial x_1} \right)^2 + m^2 + 3\lambda \phi_0(x_1)^2 \right) G(x_1, x_2) = \delta^{(4)}(x_1 - x_2). \quad (3.5)$$

The leading-order quantum correction $\langle \phi_q \rangle_{1\text{-loop}}$ obtained via (3.3) is the solution of the differential equation,

$$\left(-\left(\frac{\partial}{\partial x} \right)^2 + m^2 + 3\lambda \phi_0(x)^2 \right) \langle \phi_q(x) \rangle_{1\text{-loop}} = -3\lambda \phi_0(x) G(x, x). \quad (3.6)$$

This equation is derived by acting with the differential operator appearing on the left, on both sides of (3.3) and using the definition of the propagator G in (3.5).

It will also be useful for our purposes to write down the equation for the quantum corrected generating function $\phi = \phi_0 + \langle \phi_q \rangle_{1\text{-loop}}$. Using the fact that ϕ_0 satisfies the classical equation, $-\partial^2 \phi_0 + m^2 \phi_0 + \lambda \phi_0^3 = 0$, and that the quantum correction satisfies Eq. (3.6), it follows from combining the two, that the full generating function $\phi(x)$ is the solution to

$$-\partial^2 \phi(x) + m^2 \phi(x) + \lambda \phi(x)^3 + 3\lambda \phi_0(x) G(x, x) = 0. \quad (3.7)$$

We will ultimately need to compute $G(x, x)$ at coincident points, but for now we consider the general case of $x_1 \neq x_2$. It is convenient to use the mixed coordinate-momentum representation $G_\omega(\tau_1, \tau_2)$ for the propagator, i.e. perform the 3D Fourier transform to the 3-momentum, but keep the Euclidean time coordinate τ ,

$$G(x_1, x_2) = \int \frac{d^3 p}{(2\pi)^3} e^{i\vec{p}(\vec{x}_1 - \vec{x}_2)} G_\omega(\tau_1, \tau_2). \quad (3.8)$$

The partial differential equation (3.5) then becomes an ordinary second order differential equation,

$$\left(-\frac{d^2}{d\tau_1^2} + \omega^2 + 3\lambda \phi_0(\tau_1)^2 \right) G_\omega(\tau_1, \tau_2) = \delta(\tau_1 - \tau_2), \quad (3.9)$$

where once again,

$$\omega := \omega_p = \sqrt{\vec{p}^2 + m^2}. \quad (3.10)$$

The classical solution (2.26) entering the equation (3.9) should be Wick rotated to the Euclidean time τ . To simplify the resulting expressions, we also introduce a constant shift as in [9],

$$\tau = it + \frac{1}{m} \log \frac{\lambda z_0}{8m^2} - \frac{i\pi}{2m}, \quad (3.11)$$

which gives,

$$\phi_0(\tau) = i \sqrt{\frac{2}{\lambda}} \frac{1}{\cosh(\tau)}, \quad (3.12)$$

Thus, to determine the propagator in the classical background (3.12) one should solve the inhomogeneous second-order linear ODE,

$$\left(-\frac{d^2}{d\tau_1^2} + \omega^2 - \frac{6}{\cosh^2(\tau_1)} \right) G_\omega(\tau_1, \tau_2) = \delta(\tau_1 - \tau_2). \quad (3.13)$$

This is a textbook problem. The required solution of the inhomogeneous equation is obtained from the two solutions $f_1(\tau)$ and $f_2(\tau)$ to the corresponding homogeneous equation. The result is,

$$G_\omega(\tau_1, \tau_2) = \frac{1}{W} [\Theta(\tau_1 - \tau_2) f_1(\tau_1) f_2(\tau_2) + \Theta(\tau_2 - \tau_1) f_2(\tau_1) f_1(\tau_2)], \quad (3.14)$$

where Θ 's are the step functions and W is the Wronskian computed for the two homogeneous solutions,

$$W = \det \begin{pmatrix} f_1 & f_2 \\ f'_1 & f'_2 \end{pmatrix}. \quad (3.15)$$

The solutions of the homogeneous equation

$$\left(-\left(\frac{d}{d\tau} \right)^2 + \omega^2 - \frac{6}{\cosh^2(\tau)} \right) f_{1,2}(\tau) = 0, \quad (3.16)$$

are known [9] thanks to the identification of Eq. (3.16) as the Schrödinger equation with an exactly solvable potential. The first solution (which is regular at $\tau \rightarrow +\infty$) can be written in the form,

$$f_1(\tau) = \left(\omega^2 + 3\omega \frac{(e^{2\tau} - 1)}{e^{2\tau} + 1} + 2 - \frac{12e^{2\tau}}{(e^{2\tau} + 1)^2} \right) e^{-\omega\tau}, \quad \text{where } u = e^\tau, \quad (3.17)$$

where here and below we have temporarily set $m = 1$ to reduce the clutter. The second solution (which is regular at $\tau \rightarrow -\infty$) is obtained from $f_1(\tau)$ by the reflection of its argument, $f_2(\tau) = f_1(-\tau)$. These expressions can also be checked by a direct substitution into (3.16). Finally, the Wronskian computed for these two solutions is given by [9],

$$W = 2\omega(\omega^2 - 1)(\omega^2 - 4), \quad (3.18)$$

and is independent of the τ variable (as indeed should be the case for the second order linear ODE). Once again we remind the reader that the mass in the expressions above was rescaled to $m = 1$ (so that e.g. $\omega = \sqrt{\vec{p}^2 + 1}$ and is dimensionless), and that it can be easily recovered, when necessary, by dimensional analysis.

To find the expression for the coincident propagator $G(x, x)$ in (3.3), we must first evaluate the integral in (3.8) for $G(x + \Delta x, x)$, and then take the limit as $\Delta x \rightarrow 0$ to close the loop. However, we have to be careful with the order of limits. In fact, the momentum space integration produces a UV-finite result only at non-zero separation between the propagator end points x_1 and x_2 . When Δx does go to zero, the integral $\int d^3 p$ contains quadratically and logarithmically divergent terms and needs to be regulated. The regulated divergences are then absorbed into the renormalised parameters of the theory — the mass squared term and the coupling constant — after which the UV regulator can be removed. This was the procedure adopted in [9].

Since our main aim is to account for the effects of the Higgs explosion scale E_* , which renders the loop integrals over Euclidean 4-momenta finite, as in (2.22), we must now deviate from [9]. Our approach will be to keep a non-vanishing separation between the

space-time points, so that our integrals remain finite, before re-writing them as the integrals over d^4p . For these integrals we can implement the Higgslosion cut-off $p^2 \leq E_*^2$ directly, as in (2.20), and then safely take limit $\Delta x \rightarrow 0$ as in (2.22).

To follow the approach outlined above, we expand the integrand in (3.8) in powers of $1/\omega$, to isolate the most sensitive terms in the UV, as $p \sim \omega \rightarrow \infty$. With no loss of generality we can present (3.8) as follows:

$$G(\tau + \Delta\tau, \tau) = \int \frac{d^3p}{(2\pi)^3} e^{-\omega\Delta\tau} \frac{1}{2\omega} \left(1 + \frac{1}{\omega} A + \frac{1}{\omega^2} B + \mathcal{O}\left(\frac{1}{\omega^3}\right) \right). \quad (3.19)$$

Here we have set the non-zero separation between the space-time points to be along the time direction and kept $\Delta\tau$ positive. The factors A and B appearing on the right-hand side of (3.19) are ω -independent functions of τ and $\Delta\tau$. Using the formulae for $f_1(\tau)$, $f_2(\tau)$ and the Wronskian we find,

$$A = \frac{12e^{2\tau}}{(e^{2\tau} + 1)^2} \Delta\tau + \mathcal{O}(\Delta\tau^2) = -\frac{3\lambda}{2} \phi_0(\tau)^2 \Delta\tau + \mathcal{O}(\Delta\tau^2), \quad (3.20)$$

$$B = \frac{12e^{2\tau}}{(e^{2\tau} + 1)^2} + \mathcal{O}(\Delta\tau) = -\frac{3\lambda}{2} \phi_0(\tau)^2 + \mathcal{O}(\Delta\tau). \quad (3.21)$$

To obtain the simple form for A and B used above, we anticipate the ultimate $\Delta\tau \rightarrow 0$ limit and Taylor-expand the expressions in A and B to the first non-vanishing order in $\Delta\tau$. Note however, that while we can treat $\Delta\tau$ as a small parameter, the combination $w\Delta\tau$ is not small at high values of momenta where the exponential factor $e^{-\omega\Delta\tau}$ regulates the integrand in (3.19). This factor is therefore left unchanged.

After integrating over d^3p , the first three terms in the brackets on the right-hand side of (3.19) give rise respectively to the quadratic, linear, and logarithmic dependence on either the $1/\Delta\tau$ parameter, or on the UV cut-off momentum scale Λ_{UV} , depending on whether $\Lambda_{UV}\Delta\tau$ is $\gg 1$ or $\ll 1$. The fourth and final term in (3.19) goes as $\int dw/w^2$ and is regular in the UV at $\Delta\tau = 0$. It will be useful to represent (3.19) as follows,

$$G(\tau + \Delta\tau, \tau) = G_I + G_{II} + G_{III} + G_{\text{finite}}. \quad (3.22)$$

We can now evaluate the integrals G_I , G_{II} , G_{III} and G_{finite} . For the first integral, we have,

$$G_I(\tau + \Delta\tau, \tau) = \int \frac{d^3p}{(2\pi)^3} \frac{1}{2\omega} e^{-\omega\Delta\tau} = \int \frac{d^4p}{(2\pi)^4} \frac{1}{p^2 + m^2} e^{ip_0\Delta\tau}, \quad (3.23)$$

where we have used the familiar relation between the 4D and the 3D integrals for the free propagator,

$$\Delta_0(\tau + \Delta\tau, \tau) := \int \frac{d^4p}{(2\pi)^4} \frac{1}{p^2 + m^2} e^{ip_0\Delta\tau} = \int \frac{d^3p}{(2\pi)^3} \frac{1}{2\omega} e^{-\omega\Delta\tau}, \quad (3.24)$$

which is based on the use of the residue theorem.

For non-vanishing $\Delta\tau$ the integral is finite and does not require any UV cut-off. The expression (3.23) was derived in a theory without Higgslosion, or in the limit of infinite

Higgsplosion energy scale E_* . But since the expression on the right is the ordinary free propagator in a trivial background, we know how to modify this expression to account for the Higgsplosing self-energy. Higgsplosion is introduced exactly as in (2.20), and now we can take the limit $\Delta\tau \rightarrow 0$ and find the contribution of the first term in (3.19) to the closed loop. It is given by,

$$G_I(x, x) = \int_{p^2 \leq E_*^2} \frac{d^4 p}{(2\pi)^4} \frac{1}{p^2 + m^2} = \frac{1}{16\pi^2} \left(E_*^2 - m^2 \log \frac{E_*^2 + m^2}{m^2} \right). \quad (3.25)$$

To evaluate G_{II} and G_{III} we note the useful identity obtained by differentiating $G_I(\tau + \Delta\tau, \tau)$ on the first line in (3.23) with respect to m^2 ,

$$\frac{\partial}{\partial m^2} \int \frac{d^3 p}{(2\pi)^3} \frac{1}{2\omega} e^{-\omega\Delta\tau} = -\frac{1}{2} \int \frac{d^3 p}{(2\pi)^3} \left(\frac{1}{2\omega^2} + \frac{\Delta\tau}{2\omega^3} \right) e^{-\omega\Delta\tau}, \quad (3.26)$$

and recognising the expression on the right-hand side as precisely the sum of the integrals appearing in G_{II} and G_{III} . Since $B = 12e^{2\tau}/(e^{2\tau} + 1)^2$ and $A = B\Delta\tau$, we find that

$$G_{II} + G_{III} = -\frac{24e^{2\tau}}{(e^{2\tau} + 1)^2} \frac{\partial}{\partial m^2} G_I. \quad (3.27)$$

Differentiating our result for G_I on the right-hand side of (3.25), we find the closed-form expression for the sum of G_{II} and G_{III} at $\Delta\tau = 0$,

$$G_{II}(x, x) + G_{III}(x, x) = \frac{1}{2\pi^2} \frac{3e^{2\tau}}{(e^{2\tau} + 1)^2} \left(\log \frac{E_*^2 + m^2}{m^2} - \frac{E_*^2}{E_*^2 + m^2} \right). \quad (3.28)$$

The final term contributing to the propagator in (3.22), G_{finite} , contains no UV-sensitive contributions. It can be computed directly at $\Delta x = 0$ and one can set $E_* \rightarrow \infty$ without the need of introducing any UV cut-off. In this case we find the same expression as in [9],

$$G_{\text{finite}}(x, x) = \frac{1}{2\pi^2} \frac{6e^{2\tau}}{(e^{2\tau} + 1)^2} - \frac{6e^{4\tau}}{(e^{2\tau} + 1)^4} F, \quad (3.29)$$

where

$$F = \frac{\sqrt{3}}{2\pi^2} \left(\log \frac{2 + \sqrt{3}}{2 - \sqrt{3}} - i\pi \right). \quad (3.30)$$

Collecting the expressions for the individual contributions in equations (3.25), (3.28)-(3.29) we arrive at the final result for the propagator loop in the background field of the unbroken scalar theory with the Higgsplosion energy scale E_* . It can be slightly simplified in the limit $m^2/E_*^2 \ll 1$, where we get,

$$G(x, x) = \frac{1}{16\pi^2} \left(E_*^2 - m^2 \log \frac{E_*^2}{m^2} \right) + \frac{1}{2\pi^2} \frac{3e^{2\tau}}{(e^{2\tau} + 1)^2} \left(\log \frac{E_*^2}{m^2} + 1 \right) - \frac{6e^{4\tau}}{(e^{2\tau} + 1)^4} F, \quad (3.31)$$

or expressing everything in terms of the Brown's solution ϕ_0 , we can write an alternative equivalent representation,

$$G(x, x) = \frac{1}{16\pi^2} \left(E_*^2 - m^2 \log \frac{E_*^2}{m^2} \right) - \frac{1}{2\pi^2} \frac{3\lambda\phi_0^2}{8} \left(\log \frac{E_*^2}{m^2} + 1 \right) - \frac{3\lambda^2\phi_0^4}{32} F. \quad (3.32)$$

Recalling the defining equation (3.7) for the quantum-corrected generating functional $\phi(x)$, makes it obvious that there is a naturally occurring combination,

$$m^2\phi_0(x) + \lambda\phi_0(x)^3 + 3\lambda\phi_0(x)G(x,x). \quad (3.33)$$

It makes sense to re-absorb the first two terms on the right-hand side of (3.32) into the definitions of the renormalised coupling parameters of the theory in the following way,

$$\bar{\lambda}_* = \lambda - \frac{9\lambda^2}{8\pi^2} \left(\log \frac{E_*}{m} + \frac{1}{2} \right), \quad (3.34)$$

$$\bar{m}_*^2 = m^2 + \frac{3\lambda}{16\pi^2} \left(E_*^2 - m^2 \log \frac{E_*^2}{m^2} \right), \quad (3.35)$$

where the subscript $*$ indicates that these renormalised parameters correspond to the theory with the Higgsplosion scale E_* . Eqs. (3.34) and (3.35) define a *finite* renormalisation of the parameters, since E_* is a fixed finite non-perturbative scale of the theory; it is neither the RG scale nor the UV cut-off scale. Such finite renormalisation of the model parameters is what we would expect in the theory with Higgsplosion: such a theory does not contain UV divergences and flows to an asymptotically safe theory, where all couplings approach constant values in the UV, as was first explained in [2]. Our new results, Eqs. (3.34)-(3.35), provide a precise definition of these renormalised parameters in the UV fixed point. In Section 3.2 we will interpret these equations in terms of the running parameters and show they have the standard running with the correct slopes at low values of the RG scale, $\mu < E_*$, and flatten out and approach fixed points above the Higgsplosion scale $\mu > E_*$.

Finally, we are now in a position to compute the leading-order quantum correction $\langle\phi_q(x)\rangle_{1\text{-loop}}$ to the generating function of n -point amplitudes on multi-particle mass thresholds. The defining equation for this quantity is Eq. (3.6), and since we have already computed the propagator loop $G(x,x)$, all the quantities in this equation are known. In terms of the renormalised parameters (3.34) and (3.35), Eq. (3.6) (with \bar{m} set to 1) reads [9],

$$\left(-\frac{d^2}{d\tau^2} + 1 - \frac{24e^{2\tau}}{(e^{2\tau} + 1)^2} \right) \langle\phi_q(\tau)\rangle_{1\text{-loop}} = i 18\lambda \frac{\sqrt{8}}{\sqrt{\lambda}} F \frac{e^{5\tau}}{(e^{2\tau} + 1)^5}. \quad (3.36)$$

The solution is given by the following expression [9],

$$\langle\phi_q(\tau)\rangle_{1\text{-loop}} = -i \frac{3\lambda}{4} \frac{\sqrt{8}}{\sqrt{\lambda}} F \frac{e^{5\tau}}{(e^{2\tau} + 1)^3}, \quad (3.37)$$

which can be checked by substitution. Adding this quantum correction to the tree-level contribution $\phi_0(\tau)$, we derive the on-threshold amplitudes, cf. Eq. (2.28),

$$\langle n|\phi|0\rangle = \left(\frac{\partial}{\partial z_0} \right)^n \phi|_{z_0=0} = n! \left(\frac{\bar{\lambda}_*}{8\bar{m}_*^2} \right)^{(n-1)/2} \left(1 - \bar{\lambda}_*(n-1)(n-3) \frac{F}{16} \right). \quad (3.38)$$

This is the same expression as that derived in [9]. Where did the dependence on the Higgsplosion scale E_* go? First, it enters the definition of the renormalised coupling and mass parameters given by Eqs. (3.34)-(3.35). Secondly, there exists an additional effect,

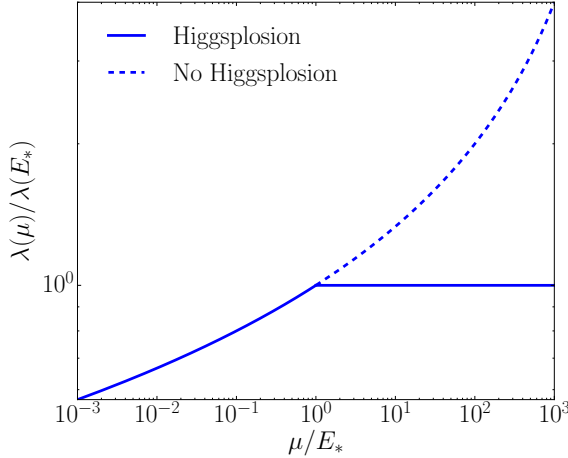


Figure 4: Running coupling $\lambda(\mu)$ in the ϕ^4 model with Higgslosion (solid line). The profile of $\lambda(\mu)$ of the same model in the absence of the Higgslosion scale is shown as the dashed line. The slope of $\lambda(\mu)$ in the presence of Higgslosion becomes flat for $\mu > E_*$ where the coupling freezes at the constant value $\bar{\lambda}_*$. This is the UV fixed point of the asymptotically safe theory.

which is the correction to the finite part F itself. Specifically, F in (3.38) is given by the expression in (3.30) plus the corrections of the order $\sim m^2/E_*^2$ which we have omitted in deriving the expression in (3.30). Section 4 is specifically dedicated to computations of finite corrections from the Higgslosion scale to precision observables.

3.2 Running couplings

In the absence of Higgslosion, i.e. in the limit where the Higgslosion scale is above some regulating UV cut-off, $\Lambda_{UV} < E_* \rightarrow \infty$, the divergent terms are absorbed into the renormalised parameters as follows,

$$\bar{\lambda} = \lambda - \frac{9\lambda^2}{8\pi^2} \left(\log \frac{\Lambda_{UV}}{m} + \frac{1}{2} \right), \quad (3.39)$$

$$\bar{m}^2 = m^2 + \frac{3\lambda}{16\pi^2} \left(\Lambda_{UV}^2 - m^2 \log \frac{\Lambda_{UV}^2}{m^2} \right). \quad (3.40)$$

These equations are fully analogous to Eqs. (3.34)-(3.35) computed in the presence of Higgslosion, except the role of E_* is now played by the UV cut-off Λ_{UV} , which is interpreted as the cut-off on the 4-momentum integration $\int d^4p$.

These expressions for the renormalised couplings have a familiar interpretation in terms of the running couplings at the RG scale μ . In the Wilsonian approach to renormalisation, one begins with the theory defined at some UV cut-off scale Λ_{UV} , where the bare parameters of the theory are specified. The UV cut-off is then lowered from Λ_{UV} to μ by integrating out all degrees of freedom in the momentum shell $\mu^2 < p^2 < \Lambda_{UV}^2$. The renormalised couplings λ and m^2 subsequently evolve to new values, specific to this RG scale μ . Hence

in order to infer the running couplings $\lambda(\mu)$ and $m^2(\mu)$ from the one-loop computation described above, one has to restrict the integration over the loop momenta to the interval $[\mu, \Lambda_{UV}]$. Adapting the expression for $\bar{\lambda}$ accordingly, ignoring the constant terms and assuming $\mu \gg m$, we find,

$$1/\lambda(\mu) = 1/\lambda(\Lambda_{UV}) + \frac{9}{8\pi^2} \int_\mu^{\Lambda_{UV}} \frac{dp}{p}. \quad (3.41)$$

This gives the well-established one-loop solution for the running coupling in $(\lambda/4)\phi^4$ theory

$$\lambda(\mu) = \frac{1}{\beta_0 \log\left(\frac{\Lambda_{LP}}{\mu}\right)} \quad , \quad \beta_0 = \frac{9}{8\pi^2}. \quad (3.42)$$

We recognise β_0 as the one-loop coefficient of the β function, $\beta(\lambda) = \frac{9}{8\pi^2} \lambda^2 + \mathcal{O}(\lambda^3)$, and the scale Λ_{LP} as the Landau pole of the ϕ^4 theory without Higgslosion. Now consider the case where Λ_{UV} is greater than the Higgslosion scale so that $E_* < \Lambda_{UV} \leq \Lambda_{LP}$. When μ exceeds E_* , we enter the Higgsploding regime and the integral contributing to $\lambda(\mu)$ ceases to grow. The β function vanishes and the coupling is frozen at $\lambda(\mu = E_*) = \bar{\lambda}_*$, the UV fixed point value given in (3.34). The resulting running of $\lambda(\mu)$ is shown in Fig. 4.

The same logic and assumptions can be applied to the running of the mass. In the absence of Higgslosion we find,

$$m^2(\mu) = m^2(\Lambda_{UV}) - \frac{3\lambda(\mu)}{16\pi^2} \left(\Lambda_{UV}^2 - \mu^2 - m^2 \log \frac{\Lambda_{UV}^2}{\mu^2} \right). \quad (3.43)$$

The expression on the right-hand side contains, as expected, quadratic and logarithmic terms depending on the UV cut-off. The quadratic terms in particular, introduce the high degree of fine tuning between the bare mass $m^2(\Lambda_{UV})$ and the radiative corrections. This is the Hierarchy problem intrinsic to QFTs with microscopic scalars. Once again, the effect of Higgslosion is to freeze the RG evolution at scales above E_* . As a result, only the so-called ‘little hierarchy’ problem remains at the scale $E_* \ll M_{Pl}$.

An even more powerful simplification comes from effect of Higgslosion on the radiative corrections to the light scalar mass, m^2 , arising from the loop of heavy degrees of freedom $M \gg E_* \gg m$. In this case [1], the radiative correction to the bare m^2 parameter is given by (cf. (3.25)),

$$\Delta m^2 = -3\lambda \int_{p^2 \leq E_*^2} \frac{d^4 p}{(2\pi)^4} \frac{1}{p^2 + M^2} \simeq \frac{-3\lambda}{16\pi^2} \frac{E_*^2}{M^2} E_*^2, \quad \text{where} \quad \frac{E_*^2}{M^2} \ll 1. \quad (3.44)$$

Returning to the model with a single degree of freedom, we are now in a position to understand the effect of Higgslosion on the end result of Section 3.1. The on-threshold $1^* \rightarrow n$ amplitude given in Eq. (3.38), now expressed in terms of the running parameters, reads,

$$\langle n|\phi|0\rangle = \left(\frac{\partial}{\partial z_0} \right)^n \phi|_{z_0=0} = n! \left(\frac{\lambda(\mu)}{8m^2(\mu)} \right)^{\frac{n-1}{2}} \left(1 - \lambda(\mu)(n-1)(n-3) \frac{F}{16} \right), \quad (3.45)$$

with the running parameters $\lambda(\mu)$ and $m^2(\mu)$ approaching constant UV fixed values at values of $\mu \geq E_*$.

Any corrections to F due to Higgslosion are of order $\sim m^2/E_*^2$ and are ignored in the equations above. The leading effect of Higgslosion enters through the modified running of the mass and coupling. We therefore expect the Higgslosion result to match the result in [9] at scales below E_* . As μ exceeds E_* , the Higgslosion result begins to deviate from [9] due to the frozen couplings.

3.3 Spontaneously broken theory

The approach in Section 3.1 can also be directly applied to the broken theory, where field ϕ acquires a VEV. Voloshin's calculation [9] for the model shown in Eq. (2.2) was extended to the broken theory by Smith [10]. The new physical scalar boson $h = \phi - \langle\phi\rangle = \phi - v$ has mass $m_h = \sqrt{2\lambda}v$ and a new 3-point coupling. Keeping only leading order shifts and assuming $\mu \gg m_h$, the renormalised parameters are given by,

$$\bar{\lambda} = \lambda - \frac{9\lambda^2}{32\pi^2} \log \frac{\Lambda_{UV}}{m_h}, \quad (3.46)$$

$$\bar{m}_h^2 = m_h^2 - \frac{3\lambda}{8\pi^2} \Lambda_{UV}^2. \quad (3.47)$$

Though some pre-factors and signs differ from the unbroken case, the degrees of divergence remain the same. The $1^* \rightarrow n$ threshold amplitude with one-loop correction can be written as,

$$\langle n|\phi|0\rangle = n! \left(\frac{\lambda(\mu)}{2m_h^2(\mu)} \right)^{(n-1)/2} (1 + \lambda(\mu) n(n-1)B), \quad (3.48)$$

where

$$B = \frac{\sqrt{3}}{8\pi}, \quad (3.49)$$

is the constant term in the broken theory, analogous to the constant $-F/16$ in the unbroken theory (see Eqs. (3.38) and (3.30)). Importantly, and in contrast to the unbroken case, the finite term B is real and the correction is positive, as discussed by Smith [10]. As before, the leading effect of Higgslosion is through the modified running couplings rather than the minor corrections to B .

3.4 Exponentiation of the one-loop corrections

It is worth noting that the exponentiation of the finite terms in the one-loop corrections to the threshold amplitudes, as derived in Ref. [8], will not be modified by the inclusion of Higgslosion. The argument used in Ref. [8] concerns only the so-called finite part of the quantum correction, and not the UV-sensitive terms where the effect of Higgslosion is manifest. Hence the entire construction presented in [8] applies equally well to Higgsploding

theories. The result for the exponentiated one-loop correction in the broken and unbroken theories respectively is,

$$\langle n|\phi|0\rangle = \begin{cases} \langle n|\phi|0\rangle_{\text{tree}} \times \exp(+n^2\lambda B) & : \text{broken theory} \\ \langle n|\phi|0\rangle_{\text{tree}} \times \exp(-n^2\lambda F/16) & : \text{unbroken theory} \end{cases} . \quad (3.50)$$

4 Precision observables in the presence of Higgslosion

Many processes in the SM occur at tree level, such as the Drell-Yan production of lepton pairs. These contain no unconstrained momenta, and thus no loop integration is required to calculate them. Only once higher-order perturbative corrections are included, do loop integrals begin to appear. Instead, we will focus on a class of observables which have no tree-level contribution. These loop-induced processes will be modified by Higgslosion at leading order, so they provide a firm testing ground for investigating Higgslosion effects.

4.1 Propagators for fermions and massive vector bosons

Expressions for Dyson-resummed propagators that take into account contributions of the self-energy, analogous to the scalar case in (2.12), can also be written down for all other massive degrees of freedom in the theory.

The renormalised fermion propagator is given by

$$S_R(\not{p}) = \frac{i}{\not{p} - m - \Sigma_{fR}(\not{p}) + i\epsilon} , \quad (4.1)$$

where m is the physical (pole) mass of the fermion and $\Sigma_{fR}(\not{p})$ is the renormalised self-energy of the fermion. Details of the definitions of the pole mass, self-energy and the renormalisation constant for the fermion field are given in the Appendix.

It is also straightforward to write down expressions for the resummed propagators for massive vector bosons in the Feynman and in the Landau gauge,

$$\text{Feynman gauge : } G_R^{\mu\nu} = -g^{\mu\nu} \frac{i}{p^2 - M^2 - \Sigma_{VR}(p^2) + i\epsilon} , \quad (4.2)$$

$$\text{Landau gauge : } G_R^{\mu\nu} = -\left(g^{\mu\nu} - \frac{p^\mu p^\nu}{p^2}\right) \frac{i}{p^2 - M^2 - \Sigma_{VR}(p^2) + i\epsilon} . \quad (4.3)$$

In both of these cases the rank-2 tensor on the right hand side of the propagator expressions does not depend on the mass parameter. The remaining factor is identical to the scalar propagator and we refer the reader to the Appendix for more detail.

All of the propagator expressions above in Eqs. (2.12) and (4.1)-(4.3) contain the factor of self-energy in the denominator. As a consequence, at $p^2 \gtrsim E_*^2$ these propagators will be suppressed by the decay width $\Gamma(p^2)$ of the propagating state into high-multiplicity final states, as in Eq. (2.15). It was explained in Ref. [2] that if the decay width of a highly virtual off-shell Higgs scalar h into multi-Higgs final states $n \times h$ Higgsplodes, it is

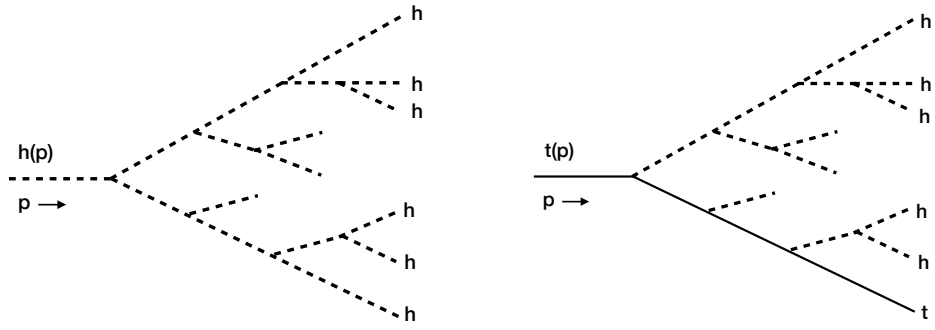


Figure 5: Emission of multiple Higgses from the single top and from the single Higgs internal line. The dominant $\sim n!$ contribution to the the decay rate at large n comes entirely from the $n \times h$ production which is essentially the same for both processes.

natural to expect that the same Higgslosion effect will occur for imaginary parts of the self-energies of any degrees of freedom X coupled to the Higgs. Indeed, at leading order in the loop expansion, there is only a single line difference between the $h \rightarrow n \times h$ process and the $X \rightarrow X + n \times h$, as shown in Fig. 5 for the example of X being the top quark.

4.2 Loop calculations for observables in the Standard Model

All the loop-induced processes that we consider arise at the one-loop level. The loop integrals which appear contain various tensor structures and denominators involving external momenta and masses. Following a similar notation to [24], the general one-loop N -point tensor integral can be written as

$$T_N^{\mu_1 \dots \mu_P}(p_1, \dots, p_{N-1}, m_0, \dots, m_{N-1}) = \frac{(2\pi\mu)^{4-d}}{i\pi^2} \int d^d k \frac{k^{\mu_1} \dots k^{\mu_P}}{D_0 \dots D_{N-1}}, \quad (4.4)$$

where the denominator contains the propagator factors

$$D_j = (k + r_j)^2 - m_j^2 + i\epsilon \quad , \quad r_j = \sum_{i=1}^j p_i \quad , \quad r_0 = 0. \quad (4.5)$$

Fig. 6 shows the general N -point function with the configuration of momenta that we use. The p_i are the external momenta of the N -point integrals, and the r_i are convenient definitions to simplify the notation. The number of spacetime dimensions in these integrals has been written as $d \equiv 4 - \epsilon$, as a precursor to performing dimensional regularisation. The general tensor integrals in Eq. (4.4) can be reduced using the Passarino-Veltman reduction procedure [25] to a set of four independent scalar integrals containing no powers of momenta in the numerators. Here, we will focus on observables which reduce to one-point, two-point

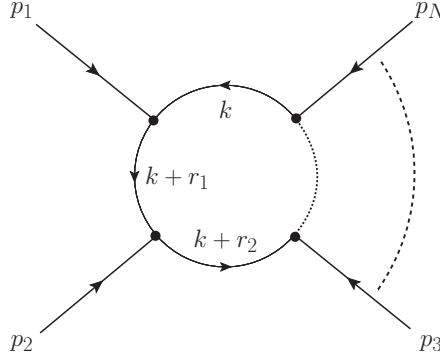


Figure 6: General N -point function showing the configuration of external and internal momenta flowing through the loop. All momenta are defined to be incoming, and the arrows show the direction of the momenta.

and three-point scalar integrals. These are:

$$A_0(m_0^2) = \frac{(2\pi\mu)^\epsilon}{i\pi^2} \int d^d k \frac{1}{k^2 - m_0^2 + i\epsilon}, \quad (4.6)$$

$$B_0(p_1^2, m_0^2, m_1^2) = \frac{(2\pi\mu)^\epsilon}{i\pi^2} \int d^d k \prod_{i=0}^1 \frac{1}{(k+r_i)^2 - m_i^2 + i\epsilon}, \quad (4.7)$$

$$C_0(p_1^2, p_2^2, r_2^2, m_0^2, m_1^2, m_2^2) = \frac{(2\pi\mu)^\epsilon}{i\pi^2} \int d^d k \prod_{i=0}^2 \frac{1}{(k+r_i)^2 - m_i^2 + i\epsilon}. \quad (4.8)$$

These integrals can be evaluated in dimensional regularisation by Feynman parameterisation, wick rotating into Euclidean space, and then carrying out the d -dimensional spherical integrals. The results are:

$$A_0(m_0^2) = m_0^2 \left(\frac{2}{\epsilon} - \gamma_E + \ln 4\pi - \ln \frac{m_0^2}{\mu^2} + 1 \right), \quad (4.9)$$

$$B_0(p_1^2, m_0^2, m_1^2) = \frac{2}{\epsilon} - \gamma_E + \ln 4\pi - \int_0^1 dx_1 \ln \frac{M_B^2}{\mu^2}, \quad (4.10)$$

$$C_0(p_1^2, p_2^2, r_2^2, m_0^2, m_1^2, m_2^2) = -\Gamma(3) \int_0^1 dx_1 \int_0^{1-x_1} dx_2 \frac{1}{2M_C^2}. \quad (4.11)$$

The dummy variables x_1 and x_2 result from Feynman parameterisation, where we have defined

$$M_B^2 = (1-x_1)m_1^2 + x_1m_2^2 + x_1(x_1-1)p_1^2, \quad (4.12)$$

for the B_0 integral, and

$$M_C^2 = (1-x_1-x_2)m_1^2 + x_1m_2^2 + x_2m_3^2 + x_1(x_1+x_2-1)p_1^2 - x_1x_2p_2^2 + x_2(x_1+x_2-1)r_2^2, \quad (4.13)$$

for the C_0 integral. The A_0 tadpole integral and the B_0 self-energy integral are UV divergent, which is manifest by the $1/\epsilon$ poles arising from dimensional regularisation. In any physical observable, these UV-divergent contributions must vanish, which is the case for all observables that we consider.

4.3 Procedure for Higgsplosion modifications to loop calculations

In the Higgsplosion framework, we begin the calculation of the loop integrals for physical processes in the same manner as for the SM. The initial starting point is that we have dimensionally regulated integrals, with the full (infinite) range of momenta allowed. One can then perform Passarino-Veltman decomposition of the tensor integrals to scalar integrals. Higgsplosion is subsequently imposed on the scalar integrals, which formally has the effect of separating the integration into two regions. Below the Higgsplosion scale, we have the unperturbed propagator of the SM and thus there is no change. Above the Higgsplosion scale, the propagator is exponentially suppressed and so the integrand rapidly goes to zero. In practice, this has the effect of restricting the allowed momenta of the integrand to $|k^2| \leq E_*^2$, where E_* is the Higgsplosion scale. The limit in which $E_* \rightarrow \infty$ corresponds to the original dimensionally regulated integrals, which would arise when performing loop calculations in the SM. The integrals can then be Wick rotated into Euclidean space, where the Higgsplosion scale becomes a Euclidean cut-off such that only momenta satisfying $k_E^2 \leq E_*^2$ are allowed. Finally, the integrations can be carried out, with numerical integrations required over the Feynman parameters. Here, we outline the explicit calculations of the UV-divergent integrals A_0 and B_0 , and the UV-finite integral C_0 .

Starting from Eq. (4.6), we perform the Wick rotation to Euclidean momenta and impose Higgsplosion by restricting the range of allowed momenta to $k^2 \leq E_*^2$,

$$A_0 = -\frac{(2\pi\mu)^\epsilon}{\pi^2} \int_{k^2 \leq E_*^2} d^d k \frac{1}{k^2 + m_0^2}. \quad (4.14)$$

We will suppress the arguments of the scalar integrals from now on, but the arguments from Eqs. (4.6)-(4.8) are implicitly assumed. Carrying out the surface integral over the d -dimensional sphere, we get

$$A_0 = -\frac{(2\pi\mu)^\epsilon}{\pi^2} \frac{2\pi^{2-\frac{\epsilon}{2}}}{\Gamma(2-\frac{\epsilon}{2})} \int_0^{E_*} dk \frac{k^{3-\epsilon}}{k^2 + m_0^2}. \quad (4.15)$$

The restriction on the momenta from Higgsplosion means that this integral is necessarily finite, so dimensional regularisation is no longer required and the $\epsilon \rightarrow 0$ limit can be taken. Finally, carrying out the k integration gives

$$A_0 = m_0^2 \log \left(\frac{E_*^2}{m_0^2} + 1 \right) - E_*^2. \quad (4.16)$$

This computation of A_0 is identical to our earlier calculation of the most singular part of the propagator in the background of the Brown solution in Section 3.1. In fact, $A_0 = -G_I(x, x)$ in Eq. (3.25).

The procedure for B_0 follows very similar steps. Starting from Eq. (4.7), after doing Feynman parameterisation and imposing Higgslosion, we get

$$\begin{aligned}
B_0 &= \frac{(2\pi\mu)^\epsilon}{\pi^2} \int_0^1 dx_1 \int_{k^2 \leq E_*^2} d^d k \frac{1}{(k^2 + M_B^2)^2}, \\
&= \frac{(2\pi\mu)^\epsilon}{\pi^2} \frac{2\pi^{2-\frac{\epsilon}{2}}}{\Gamma(2-\frac{\epsilon}{2})} \int_0^1 dx_1 \int_0^{E_*} dk \frac{k^{3-\epsilon}}{(k^2 + M_B^2)^2}, \\
&= \int_0^1 dx \left[\log \left(\frac{E_*^2}{M_B^2} + 1 \right) - \frac{E_*^2}{E_*^2 + M_B^2} \right], \tag{4.17}
\end{aligned}$$

with M_B defined in Eq. (4.12). Analogously, C_0 can be calculated starting from Eq. (4.8),

$$\begin{aligned}
C_0 &= -\frac{(2\pi\mu)^\epsilon}{\pi^2} \Gamma(3) \int_0^1 dx_1 \int_0^{1-x_1} dx_2 \int_{k^2 \leq E_*^2} d^d k \frac{1}{(k^2 + M_C^2)^3}, \\
&= -\frac{(2\pi\mu)^\epsilon}{\pi^2} \Gamma(3) \frac{2\pi^{2-\frac{\epsilon}{2}}}{\Gamma(2-\frac{\epsilon}{2})} \int_0^{E_*} dk \int_0^1 dx_1 \int_0^{1-x_1} dx_2 \frac{k^{3-\epsilon}}{(k^2 + M_C^2)^3}, \\
&= -\Gamma(3) \int_0^1 dx_1 \int_0^{1-x_1} dx_2 \frac{E_*^4}{2M_C^2(E_*^2 + M_C^2)^2}, \tag{4.18}
\end{aligned}$$

with M_C defined in Eq. (4.13). The expressions in Eqs. (4.16)-(4.18) are the final results for the scalar integrals that we use to calculate the effect of Higgslosion on precision observables.

We note here that in physical observables, the dependence on the Higgslosion scale cancels in the $E_*^2 \rightarrow \infty$ limit, which recovers the SM result. This is equivalent to the statement that when using cut-off regularisation, observables are finite in the end. The expressions describing the difference in the values of precision observables between the theory with and without Higgslosion, will have the terms $\sim E_*^2$, $\sim \log E_*^2$ and E_* -independent terms cancelled. Thus, only the terms suppressed by the inverse powers of E_* (also allowing additional logarithms) will survive from the integrals in Eqs. (4.16)-(4.18) in the results for the deviation of the observables from the Standard Model values. In the language of Section 3 this amounts to the computation of power-suppressed corrections to finite terms F and B .

4.4 Results for precision observables

Using the expressions from Eqs. (4.16)-(4.18), we can now compute the effects on precision observables induced by Higgslosion. All loop-induced observables will receive corrections that scale like $\mathcal{O}(\hat{s}/E_*^2)$. Thus, we focus on observables that can be measured to a high precision. The calculations proceed in accordance with the method outlined in the previous section, where Higgslosion is imposed after the reduction to scalar integrals. The diagram and amplitude generation is performed by **FeynArts** [26], and then the Passarino-Veltman reduction and amplitude squaring is performed by **FormCalc** [27]. The SM expressions for the loop integrals are evaluated using the **LoopTools** package.

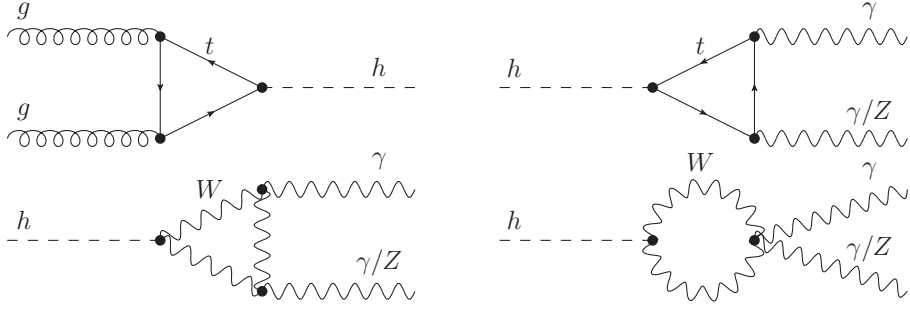


Figure 7: Leading-order Feynman diagrams for the Higgs production and decay processes $gg \rightarrow h$, $h \rightarrow \gamma\gamma$ and $h \rightarrow Z\gamma$.

4.5 Higgs precision observables

The first class of observables that we consider are the production and decay of an on-shell Higgs boson via loop-induced leading-order processes, i.e. $gg \rightarrow h$, $h \rightarrow \gamma\gamma$ and $h \rightarrow Z\gamma$. Figure 7 shows the leading-order Feynman diagrams for these processes, capturing the dominant Higgs production mechanism at the LHC, along with two of the cleanest Higgs decay modes. For the production mode, the dominant contribution comes from the top-quark loop, and we neglect the contribution from the lighter fermions. For the decay modes, there are also contributions from W -boson loops which interfere destructively with the top-quark loop.

In all three processes the external momentum scale is set by the Higgs mass, $\sqrt{\hat{s}} \simeq m_h$. This is the only external momentum scale that enters into the loop integrals for these processes, which can be decomposed into C_0 triangle integrals. To quantify the relative change due to Higgslosion, we define the quantities $\hat{\sigma}^*$ and Γ^* for the partonic cross section and decay width respectively, where the loop integrals have been calculated using the Higgslosion expressions. These are then compared to their associated SM results, and their relative differences calculated. In Figure 8, we plot the effect of Higgslosion on the Higgs observables as functions of the Higgslosion scale, E_* .

Current theoretical uncertainties on $gg \rightarrow h$ are $\mathcal{O}(10)\%$, irrespective of the center-of-mass energy of the hard process [28]. Here, a large improvement would be needed to become sensitive to the Higgslosion scenario. Even if such improvements could be achieved, the predicted experimental sensitivity is $\mathcal{O}(5)\%$ at the LHC with 3000 fb^{-1} [29]. A higher precision can be achieved for the decay $h \rightarrow gg$ at a future electron-positron collider. Ref. [30] gives a predicted precision for $\text{BR}(h \rightarrow gg)$ of 1.4% for the FCCee and 3.3% for a 250 GeV ILC.

The expected precision for $\text{BR}(h \rightarrow \gamma\gamma)$ is 3.0% at the FCCee. The rate for $\text{BR}(h \rightarrow Z\gamma)$ is too small to set tight limits at electron-positron colliders. At the HL-LHC the rate can be limited to $\mathcal{O}(10)\%$ accuracy [31]. Hence, even assuming strong improvements on the theory uncertainties and data from a future circular electron-positron collider it will not be possible to set limits on the Higgslosion scale in such measurements of a singly-produced on-shell Higgs boson.

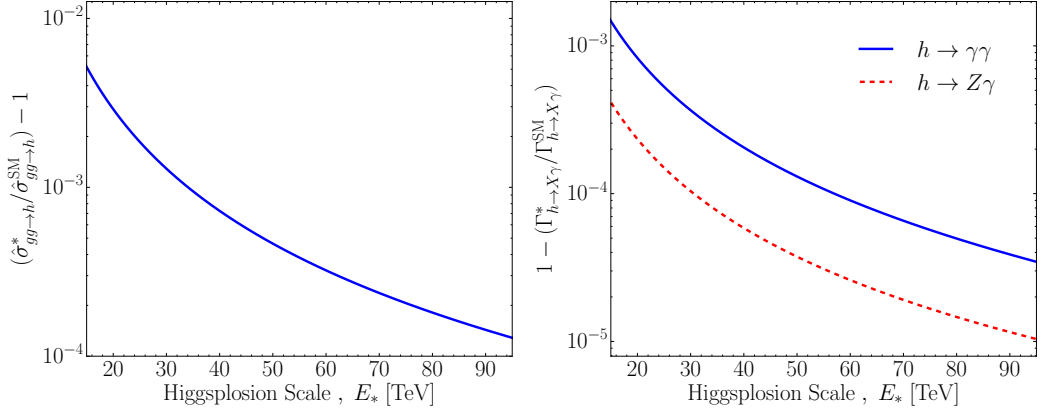


Figure 8: Plot of the effect of Higgsplosion on the partonic cross section for $gg \rightarrow h$ (left) and the partial decay width for $h \rightarrow \gamma\gamma$ and $h \rightarrow Z\gamma$ (right) as functions of the Higgsplosion scale E_* .

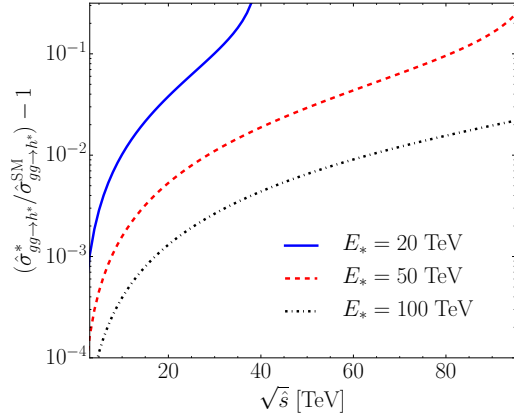


Figure 9: Plot of the effect of Higgsplosion on the partonic cross section for $gg \rightarrow h^*$ as a function of the centre-of-mass energy $\sqrt{\hat{s}}$. The different curves show different values of the Higgsplosion scale E_* .

A larger effect can be achieved by increasing the interaction scale $\sqrt{\hat{s}}$. In Fig. 9 we show the impact of Higgsplosion on the process $gg \rightarrow h^*$, when varying $\sqrt{\hat{s}}$ between 10–90 TeV. This amounts to producing a Higgs boson far away from its mass-shell or a heavy Higgs boson that could arise in an extension of the Standard Model. The effect becomes $\mathcal{O}(1)$ when $\sqrt{\hat{s}} \simeq 2E_*$, in close analogy to the $2m_t$ threshold of the $gg \rightarrow h$ process in the Standard Model. The three curves in Fig. 9 correspond to different Higgsplosion scales. As corrections from Higgsplosion scale like \hat{s}/E_*^2 , the higher the Higgsplosion scale, the large $\sqrt{\hat{s}}$ has to be to achieve an observable effect. This motivates precision studies at a future high-energy collider to test the realisation of Higgsplosion in nature.

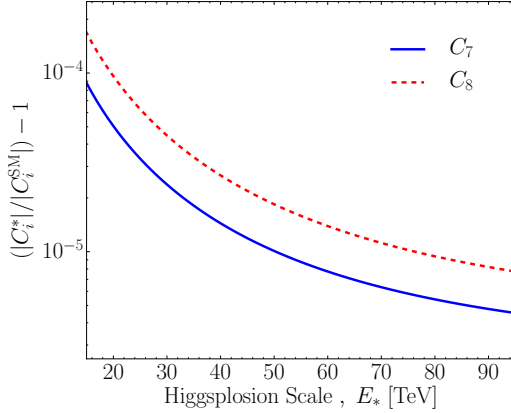


Figure 10: Plot of the effect of Higgslosion on the Wilson coefficients C_7 and C_8 for $B \rightarrow X_s\gamma$ as functions of the Higgslosion scale E_* .

4.6 Flavor observables

As Higgslosion has a direct effect on all loop-induced processes and virtual corrections, flavor observables that have been measured rather precisely could be used to set a limit on the Higgslosion scale E_* . Relevant observables include rare or semileptonic meson decays and Kaon or B -meson mixing parameters [32].

The rate of the rare inclusive decay process $B \rightarrow X_s\gamma$ is one of the most important B -physics observables as it sets stringent constraints on the parameter space of various extensions of the SM [33]. At lowest order it can be described by the transition $b \rightarrow s\gamma$. The effective Hamiltonian for this decay is usually expressed as [34]

$$\mathcal{H}_{\text{eff}} = -\frac{4G_F}{\sqrt{2}} V_{tb} V_{ts}^* \sum_{i=1}^8 C_i(\mu) \mathcal{O}_i(\mu), \quad (4.19)$$

where V_{ij} are elements of the CKM matrix, G_F is the Fermi constant and μ is the scale at which the Wilson coefficients $C_i(\mu)$ are evaluated at.

The effect of Higgslosion is predominantly encoded in the Wilson coefficients. Their relative change from the SM directly modifies the decay rate of $B \rightarrow X_s\gamma$ by the same amount. Here, we will focus on the coefficients C_7 and C_8 , which are associated with the operators

$$\mathcal{O}_7 = \frac{e}{16\pi^2} m_b \langle s_j | \omega_+ \sigma_{\mu\nu} | b_i \rangle \delta_{ij} F^{\mu\nu}, \quad (4.20)$$

$$\mathcal{O}_8 = \frac{g_s}{16\pi^2} m_b \langle s_j | \omega_+ \sigma_{\mu\nu} | b_i \rangle T_{ij}^a G_a^{\mu\nu}. \quad (4.21)$$

They are calculated from the partonic transitions $b \rightarrow s\gamma$ and $b \rightarrow sg$ respectively. Fig. 10 shows the Wilson coefficients C_7 and C_8 as functions of the Higgslosion scale, E_* .

We find that the Higgslosion modifications of $B \rightarrow X_s\gamma$ compared to the SM are small and are, even for a low Higgslosion scale of $E_* \simeq 30$ TeV, unobservable, taking theoretical and experimental uncertainties into account. Current measurements of $\text{BR}(B \rightarrow X_s\gamma) \simeq (335 \pm 15) \cdot 10^{-6}$ [35–37] are at the level of 5% accuracy only.

4.7 Anomalous magnetic dipole moment of the electron and muon

The anomalous magnetic dipole moment of the electron is one of the great successes of twentieth century physics, and QED specifically. The precision with which theoretical predictions agree with experimental measurement is about one part in a trillion, which is unprecedented for many areas of physics. However, for a muon there is a discrepancy with the SM prediction [38–41]

$$\Delta a_\mu = a_\mu^{\text{exp}} - a_\mu^{\text{theory}} \simeq 2.90 \cdot 10^{-9}, \quad (4.22)$$

which may be a sign of new physics.

The anomalous magnetic moment of a fermion quantifies how much its magnetic moment g differs from its classical value, which is predicted by the Dirac equation. This is quantified by the expression $a = (g - 2)/2$, where a is the anomalous magnetic moment. In perturbative QED, the tree level result corresponds to the vertex interaction of a charged lepton and photon at zero momentum transfer, and recovers the classical prediction. The radiative corrections to this vertex can in general be described by the form-factors F_1 and F_2 ,

$$\Gamma^\mu = F_1(q^2)\gamma^\mu + F_2(q^2)\frac{i\sigma^{\mu\nu}q_\nu}{2m}. \quad (4.23)$$

The anomalous magnetic moment is then given by $F_2(0)$. We calculate the one-loop contributions to the anomalous magnetic moment of the electron and muon and their deviations due to Higgslosion. The one-loop result for a charged lepton ℓ can be compactly written as

$$a_\ell = \frac{\alpha}{4\pi} [2B_0(m_\ell^2, 0, m_\ell^2) - B_0(0, m_\ell^2, m_\ell^2) - B_0(0, 0, m_\ell^2) - 1]. \quad (4.24)$$

In the SM at one loop, the mass dependence in the B_0 integrals cancels so the anomalous magnetic moment is $a_\ell = \alpha/(2\pi)$ for all charged leptons. However, in Higgslosion the mass dependence remains and changes are induced via the B_0 integrals. The effect of Higgslosion is shown by the plot in Fig. 11. We find that the sensitivity on a_μ has to be improved by at least two orders of magnitude to be able to set a meaningful limit on the Higgslosion scale E_* .

The anomalous magnetic moment of the electron has been measured to be [42]

$$a_e^{\text{exp}} = 11596521807.3(2.8) \cdot 10^{-13}, \quad (4.25)$$

with an experimental uncertainty of $\delta a_e^{\text{exp}} = 2.8 \cdot 10^{-13}$. Such high precision allows one to set limits on a wide range of new physics models [43]. However, as the relative changes to the anomalous magnetic moments of the electron and muon induced by Higgslosion are related by

$$\frac{1 - a_e^*/a_e^{\text{SM}}}{1 - a_\mu^*/a_\mu^{\text{SM}}} \approx \frac{m_e^2}{m_\mu^2}, \quad (4.26)$$

the increased precision for the electron compared with the muon does not translate into a better limit on the Higgslosion scale.

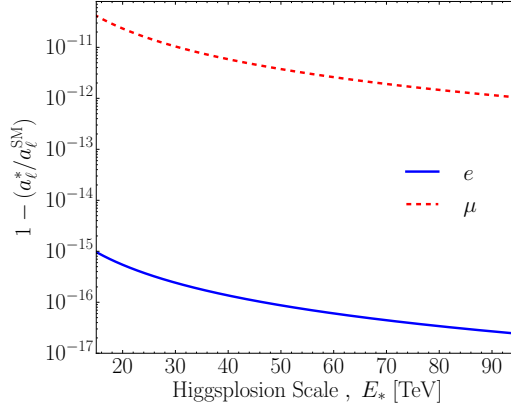


Figure 11: Plot of the effect of Higgslosion on the anomalous magnetic moment of the electron and muon as functions of the Higgslosion scale E_* .

5 Discussion and Conclusions

The motivation and main task of this paper was to provide the first detailed study of how the characteristic energy scale of Higgslosion affects the loop integrals in Higgsploding theories.

There are dramatic consequences of Higgslosion for the theory dynamics at energy scales in the UV. At the same time, we have shown that at currently accessible energies the effects of the Higgslosion scale remain very small. However, $\mathcal{O}(1)$ effects can be achieved for loop-induced processes or virtual corrections if the interactions are probed close to $\sim 2E_*$. This effect can be immediately seen in Fig. 9 for $gg \rightarrow h^*$, but it has much broader applicability. It applies to all Standard Model processes, such as Drell-Yan, multi-jet production or the production of electroweak gauge bosons.

The main features of Higgslosion that have been explored in [1, 2] and the present paper are:

1. There are no UV divergences in the theory.
2. The running of the coupling and mass parameters of the theory flattens out when the RG scale μ exceeds the Higgslosion scale E_* and the parameters reach their UV fixed points. There are no Landau poles and no couplings become negative. Therefore, the Higgsploding theory is asymptotically safe.
3. There are no hierarchically large contributions to the Higgs boson mass arising from potentially very heavy degrees of freedom with masses above E_* .
4. More generally, all particle states at energies or virtualities above E_* rapidly decay into multiple relatively soft Higgs bosons and massive vector bosons. Essentially, at $\sqrt{s} > E_*$, all elementary particle states including the Higgs itself become composite states involving high multiplicities $n \sim \sqrt{s}/m_h$ of soft electroweak quanta.

5. The self-consistency of the computational formalism, in particular the applications of the semi-classical formalism of [12] to Higgslosion [1, 15], requires that the exponentiation of the loop corrections to the tree-level Higgsploding amplitudes, originally proved in [8], remains unaffected when the loop integrations are modified by the presence of the Higgslosion scale E_* . In Section 3 we demonstrated that this is indeed the case.
6. In Section 4 we followed this up with the loop formalism in the presence of Higgslosion and computed a set of Standard Model precision observables. We found that the effects of the Higgslosion scale on these observables are small and remain unobservable at currently available energies.
7. This of course does not affect the possibility of direct observation of Higgslosion at energies \sqrt{s} above the E_* threshold [20, 44], which would potentially be achievable at future hadron colliders in the 100 TeV range, or in the early Universe (e.g. the decays and interactions of the inflaton during reheating).

It was pointed out in [1] that the direct Higgsplensive production of multiple Higgs bosons in very high energy collisions with $\sqrt{s} > E_*$ does not result in the breakdown of perturbative unitarity even when the rates appear to grow exponentially with energy. The computation of the cross section of physical processes, such as gluon fusion $gg \rightarrow n \times h$ going through an intermediate virtual Higgs boson(s) produced in the s -channel, $gg \rightarrow h^* \rightarrow n \times h$, requires the use of the dressed propagators for the intermediate h^* . This results in Higgspersion, i.e. a well-behaved cross section for arbitrary n up to very high energies [1],

$$\sigma_{gg \rightarrow n \times h}^{\Delta} \sim y_t^2 m_t^2 \log^4 \left(\frac{m_t}{\sqrt{p^2}} \right) \times \frac{1}{p^4 + m_h^4 \mathcal{R}^2} \times \mathcal{R}_n, \quad (5.1)$$

and thus

$$\sigma_{gg \rightarrow n \times h} \sim \begin{cases} \mathcal{R} & : \text{for } \sqrt{s} \leq E_* \text{ where } \mathcal{R} \lesssim 1 \\ 1/\mathcal{R} \rightarrow 0 & : \text{for } \sqrt{s} \geq E_* \text{ where } \mathcal{R} \gg 1 \end{cases}. \quad (5.2)$$

Hence, by avoiding a breakdown of perturbative unitarity in multi-boson production, the theory can retain consistency and predictivity to much higher, technically even unlimited, energy scales.

It is important to keep in mind that the expression for the cross section in (5.2) does not imply that the physical cross section once again becomes exponentially small when p^2 or s is $\gg E_*^2$. This expression was derived under the assumption that all the energy of the collision goes into producing as many soft quanta as kinematically possible. However, at energies exceeding E_* , this is no longer the case. Instead it is more advantageous for the initial highly energetic particles to emit one or few hard quanta to lower the energy from \sqrt{s} down to $\sim E_*$. The scattering then proceeds by emitting mostly soft quanta. Thus the correct behaviour for the Higgslosion cross section is that it saturates at high energies,

$$\sigma_{gg \rightarrow n \times h} \sim \begin{cases} \mathcal{R} & : \text{for } \sqrt{s} \ll E_* \text{ where } \mathcal{R} \ll 1 \\ 1 & : \text{for } \sqrt{s} \geq E_* \text{ where } \mathcal{R} \gg 1 \end{cases}. \quad (5.3)$$

This leaves the possibility of direct Higgslosion processes being observable at energies above the Higgslosion scale.

Acknowledgments

We would like to thank Claude Duhr for valuable discussions.

Appendix: Dyson-resummed propagators for fermions and massive vector bosons

The purpose of the discussion that follows is to show how the Dyson resummation of the scalar field propagator (2.12), outlined in section 2.1, applies to massive fermions and vector bosons and to derive the expressions in Eqs. (4.1)-(4.3) for the propagators of massive fermions and vector bosons quoted in section 4.1.

The unrenormalised fermion propagator with the bare mass m_0 ,

$$S(\not{p}) = \frac{i}{\not{p} - m_0 - \Sigma_f(\not{p}) + i\epsilon}, \quad (\text{A.1})$$

can be understood in perturbation theory as an infinite expansion in terms of bare propagators with the insertions of the self-energy,

$$\frac{i}{\not{p} - m_0 - \Sigma_f(\not{p})} = \frac{i}{\not{p} - m_0} + \frac{i}{\not{p} - m_0} \sum_{n=1}^{\infty} \left(-i\Sigma_f(\not{p}) \frac{i}{\not{p} - m_0} \right)^n, \quad (\text{A.2})$$

in complete analogy to the scalar propagator formula (2.4). The fermion self-energy is denoted $\Sigma_f(\not{p})$, the momentum variable \not{p} is the usual contraction with the gamma matrices, $p_\mu \gamma^\mu$, and it is also understood that $\not{p}^2 = p_\mu p^\mu = p^2$.

The physical (or pole) mass m of the fermion is defined in analogy to the scalar case in (2.7), as the value of the momentum variable $\not{p} = m \cdot 1 = m$ for which the denominator in (A.1) is zero,

$$m = m_0 + \Sigma_f(m). \quad (\text{A.3})$$

The expressions for the renormalised fermion propagator and the renormalised self-energy (*cf.* (2.10)-(2.11)) are, see for example [45],

$$S_R(\not{p}) = Z_2^{-1} S(\not{p}), \quad (\text{A.4})$$

$$\Sigma_{fR}(\not{p}) = Z_2 (\Sigma_f(\not{p}) - \Sigma_f(m)) - (Z_2 - 1)(\not{p} - m), \quad (\text{A.5})$$

where Z_2 is the renormalisation constant of the fermion field. The right-hand side of (A.5) is nothing more than a $Z_2 \Sigma_f(\not{p})$ renormalised combination with the appropriate subtractions of factors of p and m , in analogy to the scalar self-energy renormalisation condition (2.11). What makes the definition (A.5) particularly useful is the fact that it can be rearranged to give

$$\not{p} - m - \Sigma_{fR}(\not{p}) = Z_2 (\not{p} - m_0 - \Sigma_f(\not{p})), \quad (\text{A.6})$$

where we have also used the pole mass equation (A.3).

The relation (A.6) results in the following simple expression for the renormalised Dyson resummed fermion propagator,

$$S_R(\not{p}) = \frac{i}{\not{p} - m - \Sigma_{fR}(\not{p}) + i\epsilon}. \quad (\text{A.7})$$

The definition of the pole mass implies that the above expression for the renormalised propagator must have a pole at $\not{p} = m$, and the residue must be equal to i . These two conditions give,

$$\Sigma_{fR}(m) = 0, \quad (\text{A.8})$$

$$(d\Sigma_{fR}/d\not{p})|_{\not{p}=m} = 0. \quad (\text{A.9})$$

We now check what these conditions imply for the defining expression for $\Sigma_{fR}(\not{p})$ in (A.5). To do this, we Taylor expand both sides of (A.5) around $\not{p} = m$. By evaluating (A.5) at $\not{p} = m$, we find that $\Sigma_{fR}(m) = 0$, which is precisely the first condition in Eq. (A.8). The first derivative of (A.5) gives,

$$(d\Sigma_{fR}/d\not{p})|_{\not{p}=m} = Z_2 (d\Sigma_f/d\not{p})|_{\not{p}=m} + 1 - Z_2, \quad (\text{A.10})$$

and imposing the second condition, (A.9), we set the right-hand side to zero, which results in,

$$Z_2 = \left(1 - \left. \frac{d\Sigma_f}{d\not{p}} \right|_{\not{p}=m} \right)^{-1}. \quad (\text{A.11})$$

This expression fixes the renormalisation constant Z_2 in terms of the slope of the fermionic self-energy at $\not{p} = m$. This is analogous to the scalar field renormalisation constant definition we discussed before in (2.8).

Having derived the expressions for full quantum propagators of massive scalars (2.12) and massive fermions (A.7), we can follow the same route to establish the Dyson-resummed propagators of massive vector bosons. Our starting point is the expression for the bare propagator of a vector boson with a bare mass M_0 ,

$$G_0^{\mu\nu} = - \left(g^{\mu\nu} + (\xi - 1) \frac{p^\mu p^\nu}{p^2 - \xi M_0^2} \right) \frac{i}{p^2 - M_0^2 + i\epsilon}, \quad (\text{A.12})$$

where ξ is the gauge-fixing parameter. The choice $\xi = 1$ gives the Feynman gauge and $\xi = 0$ is the Landau gauge. In these two cases, the rank-2 tensor appearing on the right-hand side of the bare propagator is particularly simple as it does not depend on the mass parameter. This allows us to readily resum a geometric progression series involving a sequence of bare propagators with insertions of the vector boson self-energy.

The renormalised Dyson propagators in the Feynman and the Landau gauge are thus given by,

$$\text{Feynman gauge : } G_R^{\mu\nu} = -g^{\mu\nu} \frac{i}{p^2 - M^2 - \Sigma_{VR}(p^2) + i\epsilon}, \quad (\text{A.13})$$

$$\text{Landau gauge : } G_R^{\mu\nu} = - \left(g^{\mu\nu} - \frac{p^\mu p^\nu}{p^2} \right) \frac{i}{p^2 - M^2 - \Sigma_{VR}(p^2) + i\epsilon}, \quad (\text{A.14})$$

where M is the pole mass and $\Sigma_{VR}(p^2)$ is the renormalised self-energy of the vector boson.

The pole mass M is related to the bare mass M_0 in exactly the same way as in the scalar case (2.7),

$$M^2 - M_0^2 - \Sigma_V(M^2) = 0. \quad (\text{A.15})$$

The renormalised self-energy is defined via,

$$\Sigma_{VR}(p^2) = Z_1 (\Sigma_V(p^2) - \Sigma(M^2) - \Sigma'_V(M^2)(p^2 - M^2)), \quad (\text{A.16})$$

where $\Sigma_V(p^2)$ is the unrenormalised self-energy, and Z_1 is the field-strength renormalisation constant of the vector field. It is given by,

$$Z_1 = \left(1 - \frac{d\Sigma_V}{dp^2} \Big|_{p^2=M^2} \right)^{-1}. \quad (\text{A.17})$$

The expressions in (A.16), (A.17) are identical to those in Eqs. (2.11) and (2.8) in the scalar case.

References

- [1] V. V. Khoze and M. Spannowsky, *Higgsplosion: Solving the Hierarchy Problem via rapid decays of heavy states into multiple Higgs bosons*, *Nucl. Phys.* **B926** (2018) 95–111, [[1704.03447](#)].
- [2] V. V. Khoze and M. Spannowsky, *Higgsploding universe*, *Phys. Rev.* **D96** (2017) 075042, [[1707.01531](#)].
- [3] N. S. Manton, *Topology in the Weinberg-Salam Theory*, *Phys. Rev.* **D28** (1983) 2019.
- [4] F. R. Klinkhamer and N. S. Manton, *A Saddle Point Solution in the Weinberg-Salam Theory*, *Phys. Rev.* **D30** (1984) 2212.
- [5] L. S. Brown, *Summing tree graphs at threshold*, *Phys. Rev.* **D46** (1992) R4125–R4127, [[hep-ph/9209203](#)].
- [6] E. N. Argyres, R. H. P. Kleiss and C. G. Papadopoulos, *Amplitude estimates for multi-Higgs production at high-energies*, *Nucl. Phys.* **B391** (1993) 42–56.
- [7] M. B. Voloshin, *Estimate of the onset of nonperturbative particle production at high-energy in a scalar theory*, *Phys. Lett.* **B293** (1992) 389–394.
- [8] M. V. Libanov, V. A. Rubakov, D. T. Son and S. V. Troitsky, *Exponentiation of multiparticle amplitudes in scalar theories*, *Phys. Rev.* **D50** (1994) 7553–7569, [[hep-ph/9407381](#)].
- [9] M. B. Voloshin, *Summing one loop graphs at multiparticle threshold*, *Phys. Rev.* **D47** (1993) R357–R361, [[hep-ph/9209240](#)].
- [10] B. H. Smith, *Summing one loop graphs in a theory with broken symmetry*, *Phys. Rev.* **D47** (1993) 3518–3520, [[hep-ph/9209287](#)].
- [11] M. B. Voloshin, *Loops with heavy particles in production amplitudes for multiple Higgs bosons*, *Phys. Rev.* **D95** (2017) 113003, [[1704.07320](#)].
- [12] D. T. Son, *Semiclassical approach for multiparticle production in scalar theories*, *Nucl. Phys.* **B477** (1996) 378–406, [[hep-ph/9505338](#)].

- [13] M. V. Libanov, V. A. Rubakov and S. V. Troitsky, *Multiparticle processes and semiclassical analysis in bosonic field theories*, *Phys. Part. Nucl.* **28** (1997) 217–240.
- [14] A. S. Gorsky and M. B. Voloshin, *Nonperturbative production of multiboson states and quantum bubbles*, *Phys. Rev.* **D48** (1993) 3843–3851, [[hep-ph/9305219](#)].
- [15] V. V. Khoze, *Multiparticle production in the large λn limit: realising Higgslosion in a scalar QFT*, *JHEP* **06** (2017) 148, [[1705.04365](#)].
- [16] F. J. Dyson, *The S matrix in quantum electrodynamics*, *Phys. Rev.* **75** (1949) 1736–1755.
- [17] J. S. Schwinger, *On the Green's functions of quantized fields. 1.*, *Proc. Nat. Acad. Sci.* **37** (1951) 452–455.
- [18] J. S. Schwinger, *On the Green's functions of quantized fields. 2.*, *Proc. Nat. Acad. Sci.* **37** (1951) 455–459.
- [19] J. S. Gainer, *Measuring the Higgslosion Yield: Counting Large Higgs Multiplicities at Colliders*, [1705.00737](#).
- [20] V. V. Khoze, *Perturbative growth of high-multiplicity W, Z and Higgs production processes at high energies*, *JHEP* **03** (2015) 038, [[1411.2925](#)].
- [21] V. A. Rubakov and P. G. Tinyakov, *Towards the semiclassical calculability of high-energy instanton cross-sections*, *Phys. Lett.* **B279** (1992) 165–168.
- [22] M. V. Libanov, D. T. Son and S. V. Troitsky, *Exponentiation of multiparticle amplitudes in scalar theories. 2. Universality of the exponent*, *Phys. Rev.* **D52** (1995) 3679–3687, [[hep-ph/9503412](#)].
- [23] E. Witten, *Anti-de Sitter space and holography*, *Adv. Theor. Math. Phys.* **2** (1998) 253–291, [[hep-th/9802150](#)].
- [24] A. Denner and S. Dittmaier, *Reduction schemes for one-loop tensor integrals*, *Nucl. Phys.* **B734** (2006) 62–115, [[hep-ph/0509141](#)].
- [25] G. Passarino and M. J. G. Veltman, *One Loop Corrections for e+ e- Annihilation Into mu+ mu- in the Weinberg Model*, *Nucl. Phys.* **B160** (1979) 151–207.
- [26] T. Hahn, *Generating Feynman diagrams and amplitudes with FeynArts 3*, *Comput. Phys. Commun.* **140** (2001) 418–431, [[hep-ph/0012260](#)].
- [27] T. Hahn and M. Perez-Victoria, *Automatized one loop calculations in four-dimensions and D-dimensions*, *Comput. Phys. Commun.* **118** (1999) 153–165, [[hep-ph/9807565](#)].
- [28] R. Contino et al., *Physics at a 100 TeV pp collider: Higgs and EW symmetry breaking studies*, *CERN Yellow Report* (2017) 255–440, [[1606.09408](#)].
- [29] CMS collaboration, *Projected Performance of an Upgraded CMS Detector at the LHC and HL-LHC: Contribution to the Snowmass Process*, in *Proceedings, 2013 Community Summer Study on the Future of U.S. Particle Physics: Snowmass on the Mississippi (CSS2013): Minneapolis, MN, USA, July 29–August 6, 2013*, 2013, [1307.7135](#), <http://inspirehep.net/record/1244669/files/arXiv:1307.7135.pdf>.
- [30] J. de Blas, M. Ciuchini, E. Franco, S. Mishima, M. Pierini, L. Reina et al., *Electroweak precision observables and Higgs-boson signal strengths in the Standard Model and beyond: present and future*, *JHEP* **12** (2016) 135, [[1608.01509](#)].
- [31] J. M. No and M. Spannowsky, *A Boost to $h \rightarrow Z\gamma$: from LHC to Future e^+e^- Colliders*, *Phys. Rev.* **D95** (2017) 075027, [[1612.06626](#)].

[32] Y. Amhis et al., *Averages of b -hadron, c -hadron, and τ -lepton properties as of summer 2016*, [1612.07233](#).

[33] A. J. Buras, M. Misiak, M. Munz and S. Pokorski, *Theoretical uncertainties and phenomenological aspects of $B \rightarrow X(s)$ gamma decay*, *Nucl. Phys.* **B424** (1994) 374–398, [[hep-ph/9311345](#)].

[34] A. Ali and C. Greub, *A Profile of the final states in $B \rightarrow X(s)$ gamma and an estimate of the branching ratio $BR(B \rightarrow K^* \gamma)$* , *Phys. Lett.* **B259** (1991) 182–190.

[35] CLEO collaboration, S. Chen et al., *Branching fraction and photon energy spectrum for $b \rightarrow s\gamma$* , *Phys. Rev. Lett.* **87** (2001) 251807, [[hep-ex/0108032](#)].

[36] BELLE collaboration, A. Limosani et al., *Measurement of Inclusive Radiative B -meson Decays with a Photon Energy Threshold of 1.7-GeV*, *Phys. Rev. Lett.* **103** (2009) 241801, [[0907.1384](#)].

[37] BABAR collaboration, J. P. Lees et al., *Precision Measurement of the $B \rightarrow X_s\gamma$ Photon Energy Spectrum, Branching Fraction, and Direct CP Asymmetry $A_{CP}(B \rightarrow X_{s+d}\gamma)$* , *Phys. Rev. Lett.* **109** (2012) 191801, [[1207.2690](#)].

[38] MUON G-2 collaboration, G. W. Bennett et al., *Final Report of the Muon E821 Anomalous Magnetic Moment Measurement at BNL*, *Phys. Rev.* **D73** (2006) 072003, [[hep-ex/0602035](#)].

[39] F. Jegerlehner and A. Nyffeler, *The Muon $g-2$* , *Phys. Rept.* **477** (2009) 1–110, [[0902.3360](#)].

[40] K. Hagiwara, R. Liao, A. D. Martin, D. Nomura and T. Teubner, *$(g-2)_{\mu}$ and $\alpha(MZ2)$ re-evaluated using new precise data*, *J. Phys.* **G38** (2011) 085003, [[1105.3149](#)].

[41] M. Davier, A. Hoecker, B. Malaescu and Z. Zhang, *Reevaluation of the Hadronic Contributions to the Muon $g-2$ and to $\alpha(MZ)$* , *Eur. Phys. J.* **C71** (2011) 1515, [[1010.4180](#)].

[42] D. Hanneke, S. F. Hoogerheide and G. Gabrielse, *Cavity Control of a Single-Electron Quantum Cyclotron: Measuring the Electron Magnetic Moment*, *Phys. Rev.* **A83** (2011) 052122, [[1009.4831](#)].

[43] G. F. Giudice, P. Paradisi and M. Passera, *Testing new physics with the electron $g-2$* , *JHEP* **11** (2012) 113, [[1208.6583](#)].

[44] C. Degrande, V. V. Khoze and O. Mattelaer, *Multi-Higgs production in gluon fusion at 100 TeV*, *Phys. Rev.* **D94** (2016) 085031, [[1605.06372](#)].

[45] C. Itzykson and J. B. Zuber, *Quantum Field Theory*. International Series In Pure and Applied Physics. McGraw-Hill, New York, 1980.